# Glassy dynamics

P. LUNKENHEIMER, U. SCHNEIDER, R. BRAND and A. LOIDL

*We review dynamic processes in supercooled liquids and glasses as studied by dielectric spectroscopy. It is the only experimental technique which allows one to follow the tremendous slow-down of diffusive motion of particles in disordered condensed matter over more than 18 decades in frequency or time. The dielectric techniques used are treated in detail. As an introduction for non-specialists, the time and temperature evolution of the basic spectral features associated with various dynamic relaxation processes are discussed in detail. Among them are the structural relaxation, the occurrence of fast processes and the boson peak. The relevance of these features for glass formation is discussed. The present article may also serve as a review for recent experimental and theoretical studies on glass-forming liquids.*

## 1. Introduction

Glasses belong to the oldest materials used by mankind [1,2]. Already in prehistoric times, our early ancestors used obsidian, a volcanic glass, to manufacture knives and arrow tips. Man-made glass is believed to have first emerged in the Near East, some thousands of years BC in the form of glass beads. The first glass vessels showed up in Egypt about 1500 BC and the important discovery of glassblowing was made presumably in Phoenicia in the 1st century BC. Nowadays glasses are materials of paramount technological importance and almost ubiquitous in our daily lives, not only in the classical fields, for example architecture or packaging, but also in more recent applications, e.g. communication techniques (optical fibres) or medicine (bioactive implants). This is especially true considering the modern definition of glass as a non-crystalline solid, i.e. a state of matter, rather than the silica-based transparent material associated by everyday language to the term glass. This definition includes the large group of polymers and glass ceramics, but also more exotic materials such as amorphous metals which are believed to have a great technological future. The glass transition also plays an important role in life sciences. The continuous but dramatic slow-down of the diffusive motion of particles plays a central role in the suspension of desert insect life during drought or in avoiding freezing when the environmental temperatures fall well below the freezing point. Some arctic insects load their body fluids with a glass-forming antifreeze (e.g. glycerol) which allows these insects to supercool well below – 30°C [3].

Despite the importance of glassy materials in modern life, from a physical point of view our understanding of this state of matter is poor and the transition from the liquid to the glassy state is commonly considered as one of the great unresolved problems of condensed matter physics [4,5]. However, during recent years significant theoretical developments and experimental advances have led to a renewed interest in the physics of glasses and we may be closer to a breakthrough in the understanding of the glassy state than ever before in the long history of glass research. Most recent theoretical and experimental studies focus on the dynamic behaviour of glasses and their high-temperature precursors, the supercooled liquids. The importance of *dynamics* becomes obvious when considering the usual way of preparing a glass: a liquid has to be cooled sufficiently *fast* to avoid crystallization at the melting temperature $T_m$, leading to a supercooled liquid and finally to a glass. In fact it is almost impossible to distinguish a glass from a liquid through static properties alone, both being characterized by the absence of long-range structural order. Nevertheless, their dynamics are quite different. Let us characterize the typical dynamics of the structural rearrangement of the

*Author's address:* Experimentalphysik V, Universität Augsburg, D-86135 Augsburg, Germany.
e-mail: peter.lunkenheimer@ physik.uni-augsburg.de

molecules constituting the glass—the so-called $\alpha$-relaxation—by a relaxation time $\tau$. Going from the liquid to the glassy state, $\tau$ changes over many orders of magnitude. In contrast to the behaviour during crystallization, this change happens continuously, a phenomenon which is a prerequisite for the process of glassblowing. It is a major challenge to researchers to follow this huge change, typically spanning some 15 decades from the glass to the liquid. Also the glass transition temperature $T_g$, where the supercooled liquid forms into a solid glass, is a dynamic property: $T_g$ is often defined as the temperature where the relaxation time becomes 200 s, which is a reasonable maximum time for dynamic experiments (considering the limited patience of a typical researcher). But this time certainly depends on the average lifetime (or patience) of the observers: $T_g$ would be higher for a species of 'intelligent day-flies' (e.g. honey would be regarded as solid glass) and lower for extremely long-lived 'methuselahs' that would consider some of our polymers as liquids because they lose their form after some centuries (consider the flat spots of tires that have not moved for a long time). Even window glass may prove 'liquid', i.e. flow out of its frame, if one waits long enough [6]. The ratio of the characteristic response time of a material to the time of observation is called Deborah number, named after the Biblical prophetess Deborah, who said that the mountains flow before the Lord [7]. The understanding of structural relaxation processes and of ageing phenomena in glass-forming materials is also of great technological importance. For example, most of the modern storage devices (floppy discs, CDs, etc.) are polymer-based. Of course, one does not want to lose stored information by ageing processes after some years.

The $\alpha$-relaxation dynamics can be investigated by a variety of techniques (e.g. mechanical measurements, ac specific heat or dielectric spectroscopy) and a vast amount of data has been collected over the years. Various phenomenological and theoretical approaches have been developed to describe the experimental findings. The comparison of the temperature dependence of the $\alpha$-relaxation time with theoretical predictions states an important test for any model of the glass-transition. For most glass formers the continuous increase of the $\alpha$-relaxation time during cooling deviates significantly from thermally activated behaviour and can often be parameterized using the empirical Vogel-Fulcher-Tammann (VFT) equation [8]:

$$\tau = \tau_0 \exp\left[\frac{DT_{VF}}{T - T_{VF}}\right] \qquad (1)$$

Here D is the so-called strength parameter (see section 4.1) and $\tau_0$ is a prefactor. Thermally activated behaviour is obtained for $T_{VF} = 0$. The divergence of $\tau$ at the Vogel-Fulcher temperature $T_{VF}$ cannot be observed in real experiments. For low temperatures, the relaxation time becomes longer than the time scale of the experiment, e.g. set by the cooling rate, and the sample falls out of equilibrium. In this region $\tau(T)$ deviates from equation (1) and so-called 'ageing' phenomena show up, i.e. the dynamic response depends on the thermal history of the sample (see e.g. [9]).

The divergence of the relaxation time at $T_{VF}$, implied by the VFT equation, suggests the assumption of a phase transition at a temperature below $T_g$. The glass transition may be then closely connected to this phase transition which itself is inaccessible. This notion is supported by the so-called Kauzmann paradox relating to the entropy determined by measurements of the specific heat [1,10,11]: If the entropy of the supercooled liquid is extrapolated to low temperatures, at a temperature $T_K$, it seems to become identical to that of the crystal and even smaller for $T < T_K$. This seems very unlikely and it can be assumed that 'something happens' at $T_K$ which is often found to be of similar magnitude as $T_{VF}$. Many theories follow this notion of a low-temperature phase transition underlying the glass transition, the most prominent ones being the Adams-Gibbs theory [12,13] and the free volume theory [13–15]. Obviously, in this view of the glass transition, the low temperature region, where the glass dynamics is slow, is of great interest and consequently many early experimental studies were concerned with the slow dynamics near $T_g$.

However, during recent years the attention of many workers has switched to the fast dynamics of glass-forming materials. This was mainly stimulated by the mode coupling theory (MCT) [16–18] which is currently the most controversially discussed theoretical approach to the glass transition. MCT explains the glass transition in terms of a dynamic phase transition at a critical temperature $T_c$, significantly above the glass temperature $T_g$. In the relevant temperature region, the $\alpha$-relaxation dynamics are rather fast ($\tau \approx 10^{-10}$–$10^{-6}$ s). In addition, for the $10^{-12}$–$10^{-9}$ s time window, MCT predicts an additional contribution, now commonly termed the fast $\beta$-process. It can be visualized as a 'rattling' movement of a particle in the transient 'cage' formed by its neighbours. In contrast, the $\alpha$-relaxation is associated with the forming and decay of the cage, involving the cooperative movement of many particles. What makes MCT (and especially its simplest form, the idealized MCT) so attractive for the experimentalist is the large range of rather simple predictions, covering almost all aspects of the dynamic response of glass-forming materials. This should allow for rigid experimental tests of its validity. MCT stimulated a large variety of experimental investigations, especially of the fast dynamics of glass-forming materials, the most prominent methods used being neutron and light scattering [19–21]. But also a variety of competing theories have appeared, e.g. the coupling model (CM) [22], the frustration-limited

domain (FLD) model [23] and the model of dynamically correlated domains (DCD) [24]. Fast processes are also predicted in the CM and in a recent extension of the DCD model using the Weiss mean-field theory [25] and they are also suspected to play a role in the FLD model [23].

Dielectric spectroscopy is one of the most commonly used techniques for the investigation of the dynamic response of glass-forming materials. Essentially, the sample is subjected to an ac electrical field and the response is measured in form of a frequency-dependent complex dielectric permittivity (see section 2.1 for details). An exceptionally broad frequency range is accessible with this method, which makes it an ideal tool to follow the $\alpha$-relaxation dynamics during its many decade change from $T_g$, deep into the liquid state. Moreover, many additional contributions that play a role in the dynamics of glass formers have been detected first with this method, e.g. the presence of secondary relaxation processes (the slow $\beta$-relaxations) which are most prominent in polymers but also present in some low-molecular weight glass-formers [26,27]. Unfortunately, until recently, the region of the predicted fast processes finding so much attention during recent years, lay just at the high-frequency edge (about 10 GHz) of the range available in the best dielectric laboratories (but see [28]). First results [29 – 31] led to the conjecture that there might be no fast processes detectable with dielectric spectroscopy, which was alleged as an important point of criticism concerning the validity of MCT [5,28 – 30]. However, recent experimental advances in our group enabled us to obtain continuous dielectric spectra on glass-forming materials extending well into the relevant region [32 – 35] and the detection of fast processes in dielectric spectra of glass-forming materials is now well established. By combining classical dielectric spectroscopy, coaxial transmission, quasi-optic submillimeter and far-infrared techniques, now spectra covering more than 18 decades of frequency can be obtained extending well into the THz region [36,37]. This extremely broad dynamic window allows for the investigation of the large variety of dynamic processes present in glass-forming materials (see section 2.2) using one experimental probe only. In the present work we will provide broadband dielectric spectra on two glass-forming compounds, glycerol and propylene carbonate (PC), extending over the whole frequency range available. These two materials belong to the group of low molecular-weight organic glass-formers which are often chosen for the investigation of glass dynamics. They are relatively simple molecules with no additional side groups that complicate the relaxation process and their glass transition lies in a convenient temperature region (glycerol: $T_g \approx 185$ K, PC: $T_g \approx 159$ K). We will compare the data to those of earlier investigations with dielectric and other experimental methods. A critical comparison with the predictions of various theoretical models will be performed.

## 2. Broadband dielectric spectroscopy

### 2.1. *Basics*

The results from dielectric spectroscopy are usually presented as spectra of the real and imaginary part of the complex dielectric permittivity $\varepsilon^* = \varepsilon' - i\varepsilon''$ $\varepsilon^*$ can be defined by $D^*(\nu) = \varepsilon^* \varepsilon_0 E^*(\nu)$ with $D^*$ the dielectric displacement, $E^*$ the electric field and $\varepsilon_0$ the permittivity of vacuum. Here the star superscripts denote the use of complex quantities, a common practice to include phase information in frequency-dependent quantities [38]. The real part $\varepsilon'$ is the frequency dependent dielectric constant. The imaginary part $\varepsilon''$ is proportional to the part of $D'$ that is out of phase with the electric field with a phase difference of $\pi/2$. It is proportional to the 'loss' of energy from the applied field into the sample (in fact this energy is dissipated into heat) and therefore denoted as dielectric loss [38]. These quantities are connected to the polarization $P^*$ and the dielectric susceptibility $\chi^*$ by $P^* = \varepsilon_0 \chi^* E^*$ and $\varepsilon^* = 1 + \chi^*$.

By dielectric spectroscopy, dynamic processes can be detected that involve the reorientation of dipolar entities or the displacement of charged entities. Relaxation processes of such entities occur if they are subjected to an electric field changing with time. In many cases structural rearrangement processes are connected with such electrically active processes, e.g. the reorientation of a dipolar molecule may lead to a translational movement of its neighbours and vice versa. In this way, for instance, information on the structural $\alpha$-relaxation can be gained from dielectric measurements. Let us now consider the reaction of dipolar non-interacting molecules with a common relaxation time to the application of an electric field. If we assume that the time scale of the considered relaxation process is clearly separated from those of faster and slower processes that may be present in the material, an almost instantaneous polarization $P_\infty$ due to the fast processes will occur as shown in figure 1a. It is reasonable to assume that the dipoles will relax with a rate that is proportional to the distance from their new equilibrium orientations. For the relaxation part of the polarization $P_r$ this leads to:

$$\frac{\partial P_r(t)}{\partial t} = \frac{P_s - P(t)}{\tau} \tag{2}$$

$P_s$ is the 'static' polarization which may change further if slower processes are present. Solving equation (2) results in an exponential approach of $P_s$:

$$P := P_r + P_\infty = P_s + (P_\infty - P_s) e^{-t/\tau} \tag{3}$$

The application of a Fourier transformation leads to the following expression for the frequency-dependent dielectric permittivity:

$$\varepsilon^* = \varepsilon_\infty + \frac{\varepsilon_s - \varepsilon_\infty}{1 + i2\pi\nu\tau}, \tag{4}$$

**Figure 1. (*a*) Time dependent relaxation of the polarization in a glass former after application of an electric field at t= 0. The solid line shows the theoretical exponential response of dipolar non-interacting entities with a common relaxation time (equation (3)). The dashed line is a stretched exponential or KWW function (equation (6)), often used to describe real systems. A stretching exponent, $\beta_{KWW}$ = 0.5, was chosen. (*b*) The solid and dashed lines are the Fourier transforms of the respective curves in (*a*). For the exponential behaviour (solid line in (*a*)), a Debye response (equation (4)) is obtained. The dash-dotted line is a Cole-Davidson curve (equation (5)), often used for an empirical description of loss peaks broader than a Debye curve, with $\beta_{CD}$ = 0.5. The relaxation times and amplitudes are identical for all curves.**

shown as a solid line in figure 1b. $\varepsilon_s$ and $\varepsilon_\infty$ are the low and high frequency limits of the dielectric constant, determined by all slower and faster processes that may be present in the investigated material, respectively. Equation (4) is known as the Debye equation [39]. Resolving (4) into real and imaginary part leads to a sigmoidally shaped curve for $\varepsilon'(\log_{10}\nu)$ and to symmetric loss peaks with half widths of 1.14 decades for $\varepsilon''(\log_{10}\nu)$.

For the description of the $\alpha$-relaxation, the assumption of dipoles with identical relaxation times, relaxing independently from each other, seems unrealistic. Indeed, in most materials the Debye response, equation (4), is not sufficient to describe the experimental results and the loss peaks caused by the $\alpha$-relaxation (called $\alpha$-peaks) are broader and often asymmetric. Various modifications of equation (4) have been proposed to take account of the observed deviations [38], e.g. in the Cole-Davidson (CD) equation [38,40],

$$\varepsilon^* = \varepsilon_\infty + \frac{\varepsilon_s - \varepsilon_\infty}{(1 + i2\pi\nu\tau_{CD})^{\beta_{CD}}}, \qquad (5)$$

the addition of the exponent $\beta_{CD} < 1$ takes into account an asymmetric broadening of the loss curves at frequencies above the peak frequency $\nu_p$, as often observed in simple molecular glass formers (figure 1b). For $\nu \gg \nu_p$ the loss calculated from equation (5) follows a power law with an exponent equal to $-\beta_{CD}$.

The finding that in most materials the loss peaks are broadened in comparison with the Debye response is usually ascribed to a distribution of relaxation times. Thus an average relaxation time $<\tau>$ can be calculated. The corresponding relaxation rate will be denoted as $\nu_\tau := 1/(2\pi<\tau>)$. For the CD function, $<\tau> = \beta_{CD}\tau_{CD}$ [38]. A distribution of relaxation times may arise due to the heterogeneity of the material under investigation, caused by variations of the local environment of the relaxing entities. This heterogeneity scenario [41] has been corroborated recently by four-dimensional NMR experiments [42], dielectric hole burning [43], and photobleaching experiments [44]. An alternative scenario is that of a homogeneous non-exponential response of the relaxing entities in the time domain. This leads to deviations from Debye behaviour in the frequency domain, too. Usually the non-exponentiality is taken into account by the so-called stretched exponential or Kohlrausch-Williams-Watts (KWW) function,

$$P = P_s + (P_\infty - P_s)\exp\left[-\left(\frac{t}{\tau_{KWW}}\right)^{\beta_{KWW}}\right], \qquad (6)$$

with $\beta_{KWW} < 1$. A KWW curve with $\beta = 0.5$ is shown in figure 1a (dashed line). The KWW function was first used by Kohlrausch to describe the charge relaxation of a Leyden jar [45] and applied to dielectric relaxation by Williams and Watts [46]. This, in the beginning purely phenomenological description has been theoretically derived in a variety of models [13]. Of course, the use of the KWW function does not necessarily imply the homogeneous scenario, as equation (6) also can be transferred into a corresponding distribution of relaxation times. Fits of dielectric relaxation data in the frequency domain require a Fourier transformation of equation (6). Quite similar to the CD function, this leads to loss peaks which exhibit a power law with exponent $-\beta_{KWW}$. However, e.g. for $\beta_{CD} = \beta_{KWW}$, both functions deviate significantly, especially near $\nu_p$ (figure 1b). In the authors' experience, the CD function often describes loss data in glass-forming materials more accurately than the

KWW response [33,36,47,48] and therefore will be used in the course of the present paper.

### 2.2. *Dynamic processes*

Figure 2 represents a schematic plot of broadband loss spectra for two temperatures demonstrating the most common contributions for glass-forming materials. The $\alpha$-process leads to dominant loss peaks (indicated yellow in figure 2), shifting to high frequencies with increasing temperature. As mentioned in the introduction, in addition to the $\alpha$-relaxation, a variety of other features show up in broadband dielectric spectra of glasses and supercooled liquids. If mobile charge carriers are present, conductivity contributions lead to a $1/\nu$-divergence of $\varepsilon''(\nu)$ for low frequencies (not shown in figure 2). At frequencies some decades above $\nu_p$ the empirical functions used for the description of the $\alpha$-peak fail and an excess loss shows up (green in figure 2). In many glass formers this excess contribution can reasonably well be described as a second power law, $\varepsilon'' \sim \nu^{-b}$ with $b < \beta_{CD}$ [31,49–51]. This 'excess wing' was already noted in the early work of Davidson and Cole [40] and was found in a variety of glass-forming materials [31,49–52]. Up to now there is no commonly accepted model for the microscopic origin of the excess wing in glass-forming materials. Some intriguing scaling properties of $\alpha$-peak and excess wing were found by Nagel and coworkers [52] leading to a master curve for different temperatures and even for different materials. Moreover, using low-temperature extrapolations based on these scaling properties, the approach of $b = 0$ for a temperature near $T_{VF}$ was proposed [53]. It was argued that this constant loss behaviour could imply a divergence of the static susceptibility, again supporting speculations about a phase transition near $T_{VF}$ [53].

In many glass-forming materials, besides the $\alpha$-peak, further relaxation processes lead to additional peaks or shoulders in $\varepsilon''(\nu)$, usually located in the kHz–MHz region, as indicated in figure 2 (grey). They are termed $\beta$-relaxations (or $\gamma$, $\delta$, ... relaxations if there are more than one), sometimes with the addition 'slow' to avoid confusion with the fast $\beta$-process of MCT. Usually, the existence of two types of slow $\beta$-relaxations are assumed: The first type is ascribed to an internal change of the molecular conformation, e.g. the movement of a molecular side-group in a polymer. The second class, the so-called Johari-Goldstein $\beta$-relaxation, seems to be of more fundamental origin. This notion is based on the work of Johari and

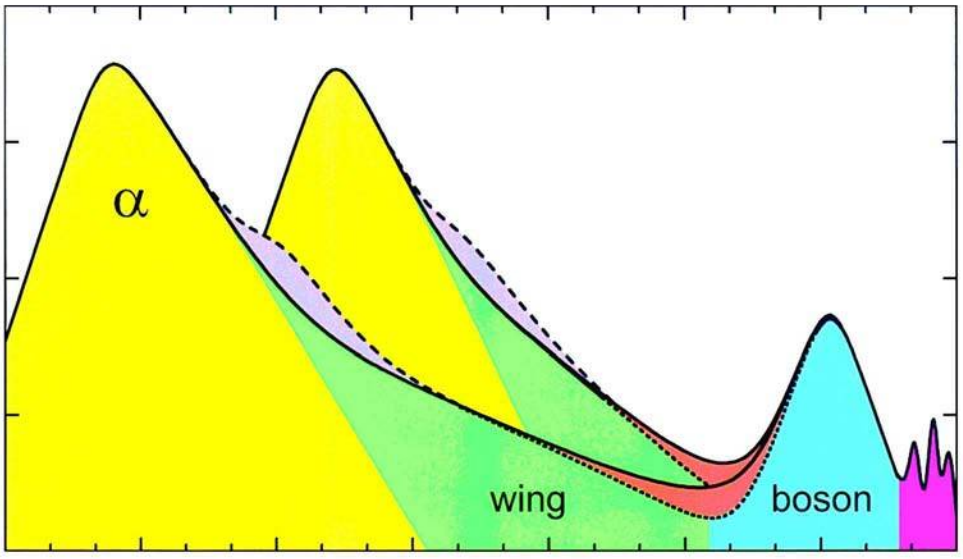


**Figure 2. Schematic view of the frequency dependent dielectric loss in glass-forming materials as observed in extremely broadband measurements. Two curves for two different temperatures are shown. Different characteristic features, not necessarily all simultaneously present in a single glass former are marked by different colours: The $\alpha$-relaxation peak (yellow), a possible $\beta$-relaxation peak (grey), the excess wing (green), the minimum with the possible contribution of an additional fast process (orange), the boson peak (blue) and the infrared bands (violet).**

Goldstein [26,27] who have demonstrated that secondary relaxation processes are a rather universal property of glass formers and can show up also in relatively simple molecular glass formers, where internal conformation changes seem unlikely. However, the microscopic processes behind this kind of $\beta$-relaxation are still controversially discussed (see e.g. [51]). It is commonly assumed that the excess wing and the Johari-Goldstein $\beta$-relaxations are due to different processes [52] and in some materials the $\beta$-relaxation may even be superimposed to the excess wing [51]. But it seems also possible that these two features are due to the same microscopic process as suggested by recent theoretical developments within the CM [54,55]. Finally, it should be mentioned that recent experiments on glass-forming Salol seem to indicate that the occurrence of a $\beta$-relaxation peak may depend on the thermal history of the sample [56].

For frequencies in the GHz-THz range, a minimum in $\varepsilon''(\nu)$ shows up. The existence of a minimum *per se* is not surprising because, after the decrease at $\nu > \nu_p$, $\varepsilon''(\nu)$ must start to increase again towards the far-infrared absorptions, well known for glass-forming materials [57,58]. However, for various glass-formers it was found that the spectral form of the $\varepsilon''(\nu)$-minimum cannot be explained by such a simple crossover [33 – 35] and fast processes contribute to $\varepsilon''(\nu)$ in this region (indicated orange in figure 2). The fast $\beta$-process predicted by MCT provides a reasonable explanation for these contributions [33 – 35,37] but other explanations may be possible [25,34,59].

At some THz another peak shows up that can be identified with the so-called boson peak known from neutron and light scattering [19 – 21,60] (blue in figure 2). The term 'boson peak' is originally defined for the scattering function S which, by means of the fluctuation-dissipation theorem [61], is in good approximation connected to the imaginary part of the susceptibility via $\chi'' = \varepsilon'' \sim S\nu$. But often the term 'boson peak' is also used for the corresponding peak in $\chi''(\nu)$ and this notation will be followed in the present work. Its name originates from the temperature dependence of its intensity, observed in the scattering experiments, which can be explained assuming boson statistics. It should be mentioned, that often the term 'boson peak' is used only to denote a high-frequency peak that is caused by vibrational excitations. In contrast, the term 'microscopic peak' is applied if the THz-peak is assumed to originate from the cage effect. Unfortunately, there is no consistent use of either expression in the literature and in the present work only the term 'boson peak' will be used.

The boson peak is a universal feature of glass-forming materials and corresponds to the commonly found excess contribution in specific heat measurements at low temperatures [11]. A variety of explanations of the boson peak have been proposed [62 – 65] but up to now there is no consensus concerning the microscopic origin of this phenomenon. Finally, in the infrared region various resonance-like features can be expected (violet in figure 2) which are due to phonon-like modes and vibrational and rotational excitations of the molecules.

### 2.3. *Experimental techniques*

In order to obtain dielectric spectra in a broad frequency range, a variety of different experimental techniques has to be combined. Figure 3 gives an overview of the techniques used in our laboratory. In principle, 21 decades of frequency can be covered. The broadest spectra on glass-forming liquids, obtained until now in this laboratory, cover more than 18 decades [36,37].

At low frequencies, up to several tens of MHz, essentially the capacitance and conductance of the sample are measured directly. The sample has to be prepared as a capacitor, as schematically indicated in figure 3. At the lowest frequencies, from $\mu$Hz up to some kHz, time-domain techniques are best suited. Here the time-dependent charging or discharging of the sample capacitor is measured after excitation with a short voltage pulse or step [66]. A Fourier transformation leads to the frequency-dependent quantities. In this way a relatively broad frequency spectrum can be obtained with one measurement only. In the region of some $\mu$Hz up to several MHz the so-called frequency response analysis can be applied. Here the sample voltage and the sample current are measured directly with a frequency response analyser using lock-in

**Figure 3. Overview of the experimental techniques and corresponding frequency ranges, employed in the dielectric laboratory at the Augsburg University. The sample geometries and the set-ups of the spectrometers are schematically indicated in the figure. The sample material is always indicated in black. Below the abscissa typical time scales and frequency bands are indicated.**

techniques. In our laboratory an impedance analyser SI1260 (Solartron, Farnborough, Hampshire, UK) in conjunction with a dielectric interface (Dielectric Instrumentation, Holt Heath, Worcestershire, UK) or an alpha-analyser (Novocontrol, Hundsangen, Germany) are available. Between several Hz and some tens of MHz autobalance bridges can be used (HP4284A (20 Hz – 1 MHz) and HP4285A (75 kHz – 30 MHz) by Hewlett–Packard, Palo-Alto, USA, in our case).

Between 1 MHz and about 10 GHz, the coaxial reflection method is best suited. Here the sample is connected to the end of a coaxial line, thereby bridging inner and outer conductor. The devices (impedance or network analysers) measure the complex reflection coefficient or perform a direct current-voltage measurement. To correct for the contributions caused by the coaxial line and connectors, a proper calibration using at least three standard impedances is necessary. In our laboratory, the Hewlett-Packard (Palo-Alto, USA) impedance analysers HP4191A (1 MHz – 1 GHz) and HP4291A (1 MHz – 1.8 GHz) and the network analyser HP8510B (45 MHz – 40 GHz) are used. The design of the sample holder and of the coaxial line, which connects the sample within the cryostat (or oven) to the measuring device, is essential in order to reach high frequencies. A variety of sample configurations for the measurement of dielectric properties with the reflection technique has been reported [67,68]. For a description of a typical coaxial line used in our laboratory, see [68].

For higher frequencies, about 100 MHz – 40 GHz, the coaxial transmission technique can be used. Here the sample material fills the space between inner and outer conductor of a coaxial line. From the transmission properties of this line, measured with a network analyser (e.g. HP8510B), the dielectric properties can be calculated. The method is based on that developed by Nicholson and Ross for time domain measurements of dielectric materials [69]. The transmission depends exponentially on the dielectric loss. Therefore, for different temperature regions lines of various lengths between 10 and 300 mm have to be used to keep the transmission within the resolution window of the network analyser.

As mentioned above, investigations of glass-forming materials in the frequency region GHz – THz are of special importance in the light of recent theoretical developments. This region can partly be covered by coaxial methods and far-infrared spectroscopy, but between some 10 and some 100 GHz measurements are difficult with these techniques. In this region resonant cavity systems can be used, but with one cavity, only a single frequency can be investigated. An alternative is given by the free-space technique where the electromagnetic wave, generated by a monochromatic source, propagates through 'free space' (i.e. is unguided) and is detected by a suitable detector after passing (or being reflected by) the sample. In principle, setups as known from optical spectrometers can be applied. In our laboratory, a quasi-optical spectrometer developed in the group of A. A. Volkov [70] is used. Its experimental arrangement is similar to that of a Mach-Zehnder interferometer. This setup allows the measurement of the frequency dependence of both the transmission and the phase shift of a monochromatic electromagnetic beam through the sample. The frequency range up to 1.2 THz is covered continuously by ten tuneable narrow-band backward-wave oscillators (BWOs). The signal is detected by a Golay cell or a pumped He bolometer and amplified using lock-in techniques. The sample is put into specially designed cells made of polished stainless steel with thin plane-parallel quartz windows; depending on the range of frequency and temperature the thickness of the sample cell has to vary between 1 mm and 30 mm. The data are analysed using optical formulae for multilayer interference [71] with the known thickness and optical parameters of the windows in order to get the complex dielectric permittivity of the sample.

In the frequency region between several hundreds of GHz and optical frequencies, commercially available infrared spectrometers can be used. In our laboratory a Fourier-transform spectrometer (IFS 113v by Bruker, Karlsruhe, Germany) is employed. Fourier-transform spectrometry does not allow the determination of the phase shift caused by the sample and usually a Kramers-Kronig transformation has to be applied to deduce the complex dielectric permittivity from the measured transmission (or reflection) data [72]. This can lead to considerable errors. However, if patterns caused by standing waves are observed in the spectrum, it may be possible to obtain information on both, real and imaginary part of the permittivity. For this purpose, the data can be analysed with standard formulas for optical multilayer interference [71].

For cooling and heating of the samples, various cryostats and ovens can be used. For ease of sample preparation it is preferable to use glass-forming materials that are liquid at, or somewhat above room temperature. In this case the use of a $N_2$-gas cryostat is best suited where the sample is subjected to a stream of cold $N_2$-gas, heated to temperatures between 100 K and 600 K. In order to avoid crystallization during the course of the measurement polished sample cells should be used, preferably made from stainless steel. Also the cooling rate should be sufficiently large, especially in temperature ranges where the tendency to crystallize is enhanced. In some cases it may be necessary to perform the measurements after heating the sample up to $T_m$ and directly cooling it to the measurement temperature with a fast rate.

To cover the complete frequency range, a single $\varepsilon''(\nu)$-curve at a given temperature is composed, using results from different setups. For some techniques the absolute values of $\varepsilon'$ and $\varepsilon''$ are not always well defined. Possible sources of error are, for example, stray capacitances, ill-

defined sample geometries or a incomplete filling of the capacitors and sample holders. Except for the transition between the HP8510B network analyser and the submillimeter wavelength spectrometer, the frequency ranges of the different devices overlap. This facilitates the matching of the curves from different devices by the application of scaling factors. In general, only one scaling factor per measurement series (with one sample, sample holder, calibration etc.) should be applied. Overall, a sufficient number of measurements, overlapping in frequency and temperature, have to be collected to minimize the errors in the composition of broadband spectra.

### 3. Broadband dielectric spectra of glass-formers

Figure 4 shows $\varepsilon'(\nu)$ and $\varepsilon''(\nu)$ of glycerol for various temperatures in the whole frequency range investigated [36]. The typical asymmetrically shaped $\alpha$-relaxation peaks shifting through the frequency window with temperature are observed in $\varepsilon''(\nu)$ (figure 4b). They are accompanied by relaxation steps in $\varepsilon'(\nu)$ as seen in figure 4a. For clarity reasons, for each temperature the spectra are shown down to about 1.5 frequency decades below the $\alpha$-peak only. For lower frequencies, conductivity contributions, most probably due to impurity ions, lead to a strong increase of $\varepsilon''$. The $\alpha$-peak can be described by the Cole-Davidson (CD) function, equation (5), as shown by the solid lines in figure 4. For comparison, a fit with the Fourier transform of the KWW function, equation (6), is shown for 204 K (dashed line) exhibiting somewhat larger deviations at high frequencies. A detailed discussion of the $\alpha$-process will be given in section 4. At frequencies $\nu > \nu_p$, $\varepsilon''(\nu)$ follows a power law $\varepsilon'' \sim \nu^{-\beta}$ (figure 4b). At higher frequencies deviations from this power law occur: For low temperatures an excess wing develops (see section 2.2) showing up as second power law, $\nu^{-b}$ with $b < \beta$ before the minimum region is reached. The exponent b increases with increasing temperature and at high temperatures, $T \geqslant 273$ K, the excess wing seems to have merged with the $\alpha$-peak. The excess wing is accompanied by an additional decrease in $\varepsilon'(\nu)$ as can be inferred from figure 4a. The excess wing will be discussed in detail in section 5.

In the GHz to THz frequency range the $\varepsilon''(\nu)$-minimum, first reported in [33], shows up (figure 4b). With decreasing temperature, its amplitude and frequency position decreases and it becomes significantly broader. Finally, near 2 THz a peak is observed. The peak frequency is temperature independent within experimental error and its amplitude increases with temperature. This peak is located at the same frequency as that found in light and neutron scattering experiments [73] and hence can be identified with the boson peak (section 2.2). Corresponding to the peak in $\varepsilon''(\nu)$, $\varepsilon'(\nu)$ exhibits a decrease near 1 THz (figure 4a).

In figure 5 the loss spectra for glycerol and PC [37] are shown in a three-dimensional representation. In both materials the spectra show the same overall behaviour with the succession of $\alpha$-peak, excess wing, minimum and boson peak. The lines in figure 5 indicate peak positions and transition points between different characteristic regions in the spectra. For both materials the dramatic increase of the $\alpha$-relaxation timescale at low temperatures leads to a strong shift of the $\alpha$-peak towards low frequencies. In contrast the boson peak position seems to be nearly constant. The shallowness of the minimum region is clearly seen in these plots. The slope of the excess wing, constituting the low-frequency wing of the minimum, increases with temperature. For high temperatures ($T \geqslant 273$ K for glycerol and $T \geqslant 193$ K for PC) it merges with the $\alpha$-peak. But also a qualitative difference of both materials shows up in figure 5, in the region between minimum and boson peak: For glycerol the minimum is followed

**Figure 4. Frequency dependence of the dielectric constant (*a*) and the dielectric loss in glycerol at various temperatures [36]. The solid lines are fits with the CD function (equation (5)) the dashed lines are fits with the Fourier transform of the KWW law (equation (6)) both performed simultaneously on $\varepsilon'$ and $\varepsilon''$ (for clarity the latter is shown for one temperature only, see [49]). The $\alpha$-response, well described by the CD function, is seen shifting over many decades of frequency with temperature. In addition, in the loss (*b*), the excess wing, minimum and boson peak show up. Note that the boson peak (near 1 THz) seems to be superimposed on the shallow minimum.**

by a shallow increase to which a much steeper increase towards the boson peak seems to be superimposed. In contrast, in PC the high-frequency wing of the minimum simultaneously forms the low-frequency wing of the boson peak and $\varepsilon''(\nu)$ increases much weaker towards the boson peak (see section 6.3).

## 4. The α-process

### 4.1. *Relaxation time*

The most significant result of an analysis of the α-relaxation process is the temperature dependence of the α-relaxation time. For glycerol and PC, vast number of measurements of

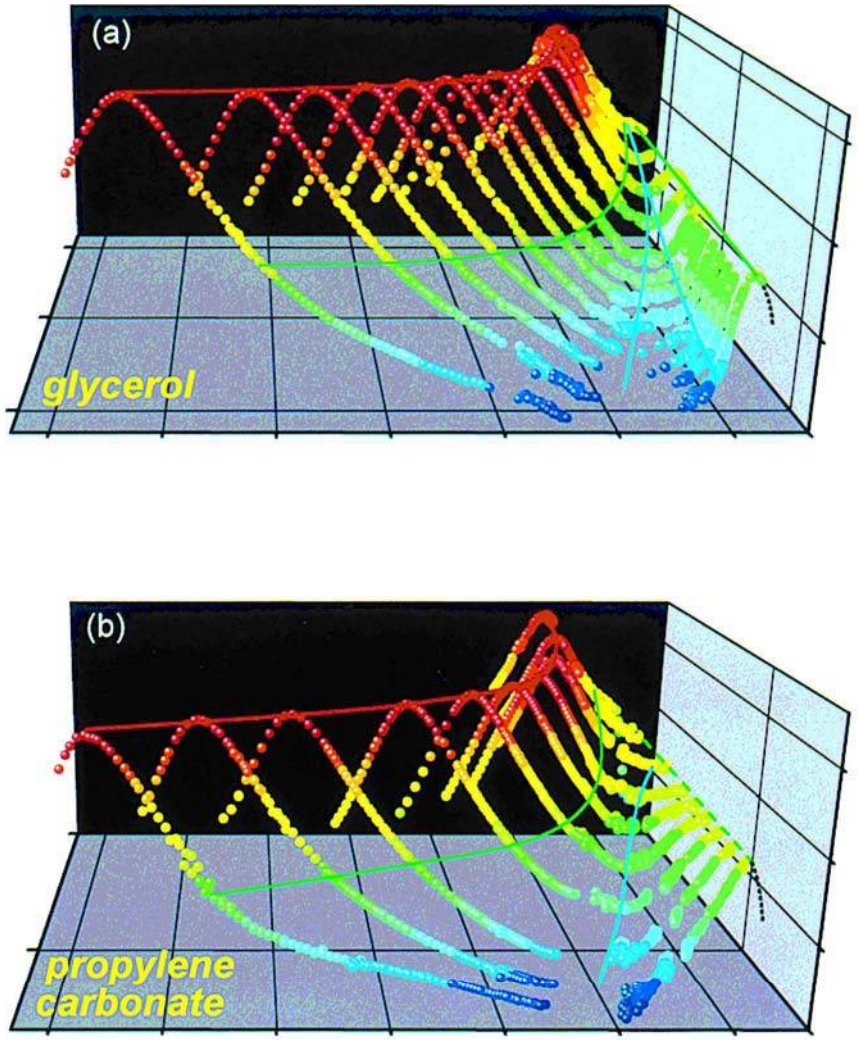


**Figure 5. Three-dimensional plot of the dielectric loss of glycerol (*a*) and PC (*b*) in dependence of temperature and frequency. The lines guide the eyes connecting characteristic points of the loss curves: the α-peak, the change of slope at the transition to the excess wing, the minimum, the onset of the steeper increase towards the boson peak (for glycerol only) and the boson peak (tentatively, because actually measured at four temperatures for glycerol and at room temperature for PC, only). The black dotted lines show a reasonable extrapolation of the boson peak at the lowest temperature, based on the room temperature measurements. The dramatic slowing down of the α-relaxation shows up in the strong shift of the α-peak towards low frequencies with decreasing temperature. In contrast the boson peak seems to be nearly temperature independent. It is obvious that the excess wing merges with the α-peak at high temperatures. The amplitude and frequency of the minimum increases with temperature. Note the different behaviour of glycerol and PC in the transition region between minimum and boson peak.**

the $\alpha$-relaxation time have been reported in literature. The $\tau$(T)-results from various dielectric investigations [26,29,31,40,58,74 – 81] have been digitized and are shown, together with the results of the present work, in an Arrhenius representation (figure 6). If available, the average relaxation time $<\tau>$ is plotted. In most other cases, $\tau$ was calculated from the peak frequency, which for most spectral forms is a good estimate for $1/(2\pi<\tau>)$. In Kudliks work [74], $<\tau>$ was obtained from fits with a modified CD function that takes account of the excess wing. Payne and Theodorou [77] obtained $\tau$(T) by assuming a Debye behaviour and making certain assumptions for the relaxation strength. Overall, the data agree rather well but some deviations of the data sets from different sources, typically up to a factor of 2, are present. As commonly found for most glass-forming liquids, for both materials the $\tau$(T) curves deviate significantly from simply thermally activated behaviour leading to a pronounced curvature in the Arrhenius representation of figure 6.

The lines in figure 6 are fits of the $\tau$(T)-curves of both materials with a VFT law, equation (1). For glycerol, $T_{VF}$ = 129 K, $\nu_0 = 1.1 \times 10^{14}$Hz and D = 17.9. For PC, $T_{VF}$ = 136 K, $\nu_0 = 4.1 \times 10^{11}$ Hz and D = 5.1 (the obviously erroneous point of Payne and Theodorou [77] at $1000/T \approx 5.1$ K$^{-1}$ was not used for these fits). The strength parameter D can be used to classify glass formers according to the deviation of their $\tau$(T) curves from thermally activated behaviour [82]: The so-called 'fragile' glass formers reveal small values of D (typically D < 10), with large deviations; the 'strong' glass formers (D > 10) follow an Arrhenius law more closely. The strength parameters resulting from the fits in figure 6 indicate that glycerol (D = 17.9) is a rather strong and PC (D = 5.1) is a fragile glass former. This classification scheme has proven very useful as many properties of glass-forming materials are correlated with their strength or fragility. Only small deviations from the empirical VFT formula show up for glycerol at high temperatures (figure 6a) in accord with earlier investigations [31,81,83]. In contrast, for PC the deviations are greater. A similar behaviour was seen in earlier works [29,79] where a low-temperature VFT behaviour with a transition to thermally activated behaviour above a temperature $T_A$ was suggested. $T_A$ was interpreted as the temperature below which the potential energy landscape in configuration space becomes important [80]. However, it must be stated that alternative descriptions are also possible, for example using VFT behaviour at high temperatures, and a thermally activated behaviour at low temperatures; or a combination of VFT functions [84].

To resolve these ambiguities, Stickel *et al.* [79,85] proposed a derivative analysis method. Plotting

$$d := \left[ \frac{-d \log_{10} \nu_\tau}{d(1/T)} \right]^{-1/2} \qquad (7)$$

*vs.* T leads to a linearization of the VFT equation while for the Arrhenius case a constant is obtained. These 'Stickel plots' for glycerol and PC are shown in the insets of figure 6. To take advantage of the large database available in glycerol and PC, Stickel's method was applied to a high-order polynomial fit of all data of figures 6a and b. This significantly reduces the large scattering of data points generated by the calculation of derivatives†. The solid lines in these plots are the transferred VFT-curves of the main

**Figure 6. Arrhenius representations of the temperature dependent relaxation times of glycerol (*a*) and PC (*b*) as reported from various dielectric measurements including the present work (solid circles). For glycerol (*a*), data from the following references are included: [31] (diamonds), [40] (crosses), [58] (stars), [74] (triangles), and [81] (pluses). For PC (*b*) data from [29] (open diamonds), [26] (filled triangles), [74] (open triangles), [75] (filled squares), [76] (filled diamonds), [77] (stars), [79] (open squares) and [80] (crosses) are shown. The solid lines are fits with a VFT behaviour, equation (1). The insets show the derivative plots of the $\nu_\tau$(T) data of glycerol as suggested by Stickel *et al.* [79,85]. d is defined in equation (7). Stickel's method was applied to a polynomial fit of all data of the main frames. This kind of plot makes a VFT curve linear and for thermally activated behaviour a constant is obtained. The solid lines are calculated with the same parameters as the VFT fits in the main frames.**

†A 7$^{th}$-order polynomial was used, but also higher order polynomials were tested to exclude possible artefacts due to the choice of the fitting function. Except for some small deviations at the highest temperatures the qualitative behaviour is independent of the fitting function.

frames. The deviations, seen only weakly in the conventional plot, become more pronounced in this representation. For glycerol (inset of figure 6a) a linear region for $T < 285$ K ($1000/T \approx 3.5$ K$^{-1}$) is observed, similar to the findings in [86]. It indicates a good description with the VFT law in this region, in agreement with the fit in the main frame. However, above this temperature the behaviour becomes complicated and no further significant VFT or Arrhenius regions can be identified. For PC (inset of figure 6b), significant deviations from linear behaviour are detected in the whole temperature region and clear VFT and Arrhenius regions are not observed. This is at variance with the suspected succession of two VFT and an Arrhenius region in [85], where, due to the stronger scattering of the data the continuous curvature revealed by the present results was not detected.

Overall, for both materials the VFT function is not able to describe the data in the whole temperature range and the Stickel-plots suggest a rather complex behaviour with a crossover between various regions of different temperature characteristics of $\tau(T)$. One has to mention that the significance of the results of Stickels method is not quite clear. For example, for glass-forming Salol an analysis with Stickels method [79] and an alternative analysis with the VFT function in a sliding frequency window [84] yielded inconsistent results. It was argued [87] that a test of fitting formulas and theories using the derivatives of measured quantities may not be justified.

Aside from the above more or less phenomenological descriptions of the temperature dependence of the $\alpha$-relaxation time, there is a variety of predictions from different competing microscopic theories. However, the experimental results often can be described with nearly equal quality by quite different theoretical models and it has proven extremely difficult to arrive at a final decision in favour or against a specific model from fits of $\tau(T)$ alone. For example, the present data on PC have been demonstrated [37] to be adequately described by an extended free volume theory [15] and by the FLD theory [23], despite both models involving very different transition temperatures near $T_g$ and above $T_m$, respectively. In the present work we therefore refrain from providing an extensive analysis of our data with microscopic approaches.

### 4.2. *Width parameter*

Besides the relaxation time, the $\alpha$-response is characterized by its relaxation strength $\Delta\varepsilon$ and a width parameter. For the latter usually an exponent $\beta$ (e.g. $\beta_{CD}$ or $\beta_{KWW}$) is used, determined from fits of the $\alpha$-peaks as mentioned in section 2.1. Obtaining precise values of $\beta(T)$ is a difficult task as there are various sources of error in its determination (e.g. $\beta$ depends critically on the choice of the frequency region used for the fits). In addition, when the loss peaks shift towards the high frequency limit of the available frequency window, the error for $\beta$ is enhanced as successively fewer data points are available at the high-frequency side of the $\alpha$-peaks. Concerning the high-temperature behaviour of the shape parameter $\beta$, there is some dispute in the literature, caused mainly by inconsistent results from dielectric spectroscopy and other methods as for example light scattering [see 29,30,52,78,88]. The high-temperature behaviour of $\beta$ is of interest as the MCT makes distinct predictions for $\beta(T)$: Above $T_c$, $\beta(T)$ should reveal a temperature independent value, smaller than unity. This is in contrast to the plausible notion that $\beta(T)$ should approach unity, deep in the liquid state because, due to the fast thermal fluctuations, each relaxing entity 'sees' the same environment, leading to a Debye response. From various investigations, most of them performed by light scattering [e.g. 78,88–91], a nearly constant $\beta(T)$ was deduced. But also the contrary was found [92], especially in dielectric experiments [e.g. 29–31] and considered as evidence against the validity of MCT. In contrast to the present results, the dynamic region accessed in these dielectric experiments was restricted to frequencies below about 10 GHz.

In figure 7 the temperature dependence of $\beta_{CD}$ of glycerol and PC is shown. For comparison, the results from a variety of dielectric investigations of glycerol taken from literature are included [29,40,74–77,80,81,93]. At low temperatures the data match reasonably well. For $\beta(T)$ a linear increase up to about 300 K for glycerol and up to about 200 K for PC can be stated. Based on the data from the present work, at higher temperatures $\beta(T)$ tends to level off at $\beta \approx 0.75$ for glycerol and $\beta \approx 0.9$ for PC. This finding seems to be in contrast to the results from other dielectric investigations [29,31] but at high temperatures their data points have a large uncertainty as there the $\alpha$-peak approaches the high-frequency limit of their experimental setup (about 10 GHz). In contrast, the value of $\beta_{CD} = 0.904$ at 298 K deduced by Barthel *et al.* [75] for PC (square in figure 7b) was obtained from high-frequency dielectric measurements at 0.95–89 GHz.

Overall, in both glycerol and PC, a tendency of $\beta_{CD}(T)$ to level off at a constant high-temperature value, smaller than unity, is observed. This finding agrees at least qualitatively with the MCT-prediction of a constant non-Debye behaviour at high temperatures. One has to note that the observed saturation of $\beta(T)$ seems to occur at temperatures somewhat higher than the $T_c$ determined for these materials (252 K for glycerol and 187 K for PC, section 6.1). However, a reasonable description of the $\alpha$-peaks for $T > T_c$ is also possible with a constant $\beta_{CD} = 0.63$ for glycerol [47] and $\beta_{CD} = 0.8$ for PC.

The third parameter characterizing the $\alpha$-relaxation is its relaxation strength. In dielectric spectroscopy it is measured by $\Delta\varepsilon := \varepsilon_s - \varepsilon_\infty$. However, its temperature dependence is often dominated by dipolar interactions or correlation effects and an unambiguous comparison with theoretical predictions is difficult. Therefore it will not be considered further in the present work and the reader is referred to [36,37].

## 5. The excess wing

A well developed excess wing shows up in the spectra of glycerol and PC (figures 4 and 5). Besides the scaling approach, noted in section 2.2, a variety of alternative descriptions of this feature were proposed. Recently, some phenomenological functions have been developed that are able to take account of both the $\alpha$-peak and the excess wing [51]. In addition, it is possible to describe the $\alpha$-peak including the wing at least partly using the FLD model [23] and the DCD model [24]. Recently it was shown that the spectra of glycerol, presented here, can be fitted well up into the minimum region, by a combination of the DCD and the Weiss mean-field theory [25]. Finally, it was shown [31,55,94] that the excess wing can also be described by a $\beta$-relaxation process, nearly masked by the dominating $\alpha$-process. This notion may find an explanation within the framework of the CM [54,55]. However, overall there is no commonly accepted explanation for this feature and it is still considered as one of the great mysteries in the properties of glass-forming materials.

The (purely phenomenological) description of the excess wing, finding most attention, is given by the so-called Nagel-scaling [30]. Nagel and coworkers found that the $\varepsilon''(\nu)$-curves for different temperatures and even for different materials, including the wing, can be scaled onto one master curve by plotting

$$Y := w^{-1}\log_{10}\frac{\varepsilon'' \nu_p}{\Delta\varepsilon\nu} \quad vs. \quad X := \frac{w^{-1}}{1+w^{-1}}\log_{10}\frac{\nu}{\nu_p}. \qquad (8)$$

Here w denotes the half-width of the loss peak, normalized to that of a Debye-peak, $\nu_p$ is the $\alpha$-peak frequency and $\Delta\varepsilon$ the relaxation strength.

In figure 8 the present data for glycerol and PC are shown, scaled according to equation (8). To maintain readability, for each material curves for three different temperatures only are shown. In addition, only data points up to the onset of the $\varepsilon''(\nu)$ minimum are included and no corrections for conductivity contributions have been performed (for some discussions concerning this point,

**Figure 7. Temperature dependence of the $\alpha$-peak width-parameter $\beta_{CD}$ of glycerol (*a*) and PC (*b*) as determined from simultaneous fits of $\varepsilon'(\nu)$ and $\varepsilon''(\nu)$ with the CD-function, equation (5) (figure 4 and [37]). In addition to the present results (circles), the following results from earlier dielectric investigations reported in literature are included. (*a*) [31] (crosses), [40] (diamonds), [74] (triangles). (*b* ). [29] (crosses), [74] (triangles), [75] (square). The $\beta$(T) of Kudlik [74] was determined from fits with a modified CD function that takes account of the excess wing. The dashed lines are drawn to guide the eye. Note the tendency of $\beta$(T) to saturate at high temperatures.**

**Figure 8. Frequency dependent dielectric-loss ($\varepsilon''(\nu)$) of glycerol at 195 K, 223 K and 363 K (circles) and PC at 158 K, 173 K and 253 K (triangles), scaled according to Nagel and coworkers [52] (equation (8)). w denotes the half-width of the loss peaks, normalized to that of a Debye-peak, $\nu_p$ is the $\alpha$-peak frequency and $\Delta\varepsilon$ the relaxation strength. For abscissa values X < 9, the data fall onto one master curve. For higher values of X, some small deviations from a single master curve are seen (see inset for a magnified view of the high-X region).**

see [95]). The present plot reveals a good scaling of the data at not too high values of X. At very high values of X small deviations from a single master curve show up (see inset) which, however, are just at the edge of the experimental resolution. Overall it is very intriguing to see such different spectra from different materials collapse onto one curve. During the last years some criticism of the Nagel-scaling arose concerning its universality and accuracy [96–98] and minor modifications of the original scaling procedure have been proposed [98]. However, it is still commonly believed that the Nagel-scaling is of significance for our understanding of glass-forming liquids and many efforts have been made to check for its validity in a variety of materials [81,96–101].

At this point it may be mentioned that the Nagel scaling is not a universal property of disordered systems in general, in contrast to previous assumptions [99]. Recently it was shown [100] that the excess wing is absent in various 'plastic crystals', a class of materials which are characterized by disorder with respect to the *orientational* degrees of freedom of the translationally ordered molecules. Plastic crystals are often considered as model systems for 'conventional' glass formers and, except for the absence of the excess wing, their properties resemble that of glass-forming liquids in many respects.

The Nagel scaling strongly suggests a correlation of $\alpha$-peak and excess wing parameters, especially of $\beta$, the power-law exponent at $\nu > \nu_p$, and b, the wing exponent. It was proposed [50,53] that b should become zero for a limiting value of $\beta^* \approx 0.38$ or $w = 2.6$[‡]. As the static susceptibility is proportional to the area under the $\alpha$-peak, it was argued that this possible constant loss behaviour would imply a divergence of the static susceptibility. By a low-temperature extrapolation of w(T)-curves of various glass-formers, Nagel and coworkers suggested that this limit is reached near the Vogel-Fulcher temperature $T_{VF}$ [53]. This finding supports speculations about a phase transition from the liquid to the glass state, underlying the glass transition. In addition, a divergent susceptibility was also deduced directly from an extrapolation of b to low temperatures, which for various glass formers indeed seems to approach zero near $T_{VF}$ [50].

Figure 9 shows the temperature dependence of $\beta_{CD}$ for glycerol and PC. $T_{VF}$ is indicated by the dashed lines. A linear extrapolation of $\beta_{CD}(T)$ leads to values of $\beta(T_{VF})$ clearly larger than $\beta^*$ and a change of the temperature characteristics at low temperatures has to be assumed to obtain $\beta(T_{VF}) = 0.38$.

The above procedure enables an investigation of the excess wing exponent by the more simple determination of the $\alpha$-peak width parameter $\beta$. A more direct way to check for a divergent static susceptibility is the investigation of the temperature dependence of the exponent b itself. However, an unambiguous determination of b is difficult, especially at higher temperatures, where $\alpha$-peak, wing, and the minimum strongly overlap in frequency. For this purpose, a parameterization using the sum of two power laws, $\varepsilon'' \sim c_\beta \nu^{-\beta} + c_b \nu^{-b}$ was used in [50]. In order to take into account the additional contributions in the minimum region and the increase towards the boson peak, a constant loss and two power laws can be added [59] which enables to obtain information on b(T) up to relatively high temperatures. The resulting b(T) (figure 9) can be reasonably well extrapolated to zero at $T_{VF}$, similar to the findings in [50]. While for glycerol the significance of this extrapolation is low, the results for PC indeed seem to support the approach

**Figure 9. Temperature dependence of the $\alpha$-peak width-parameter $\beta_{CD}$ (open circles) and *b* (squares) for glycerol (*a*) and PC (*b*). b is obtained from fits with a phenomenological ansatz comprising a sum of two power laws for the high-frequency wing of the $\alpha$-peak and some additional contributions for the $\varepsilon''(\nu)$-minimum [59]. The solid lines demonstrate a possible extrapolation to $b(T_{VF}) = 0$ which may indicate a divergent susceptibility at $T_{VF}$. $T_{VF}$ (from the VFT fits in figure 6) is indicated by the dashed lines. The insets show the prefactor of the power law $c_b \nu^{-b}$ used for the description of the excess wing. The dotted lines demonstrate that it is not possible to draw definite conclusions concerning a non-zero value of $c_b$ at $T_{VF}$.**

‡For some remarks concerning the justification of this assumption, see [101].

of a constant loss at $T_{VF}$. However, as already noted in [50], even if b becomes zero, a divergent susceptibility will only be reached, if the prefactor $c_b(T)$ does not approach zero for $T \rightarrow T_{VF}$. $c_b(T)$ for both materials is shown in the insets of figure 9. As indicated by the dotted lines, a definite statement concerning this point is not possible. The same conclusion can be drawn from the results on $c_b$ shown in [50]. Overall, no clear evidence for a divergent susceptibility at low temperatures can be deduced from an investigation of the temperature evolution of the excess wing.

## 6. The fast dynamics

### 6.1. $\varepsilon''(\nu)$ minimum

In figure 10, a magnified view of the high-frequency region of $\varepsilon''(\nu)$ is shown for both materials. The most naive assumption for the spectral form of the dielectric loss in the minimum region is a simple crossover from the $\alpha$-peak or the excess wing to the boson peak. For the low frequency wing of the boson peak a linear or superlinear increase is commonly found for a variety of glass-formers [19,20,57]. Indeed, for the lowest temperatures investigated, where the boson peak contributions can be assumed to become dominant, a linear increase for PC and even a superlinear increase of $\varepsilon''(\nu)$ for glycerol is approached (for further comments, see section 6.3). Therefore in the inset of figure 10 the simple postulate

$$\varepsilon'' = c_b \nu^{-b} + c_n \nu^n \qquad (9)$$

with $b < 1$ and $n = 1$ is used to analyse the data; b was chosen to match the power law seen in $\varepsilon''(\nu)$ between 1 GHz and the minimum. Clearly there is no way to obtain a reasonable fit of the rather shallow $\varepsilon''(\nu)$-minima in this way. Independent from any model assumptions, this empirical result provides clear experimental evidence that in the region of the $\varepsilon''(\nu)$-minimum additional fast processes contribute significantly to the dynamics of the investigated glass-forming materials. *We consider this finding as the most important outcome of our high-frequency dielectric investigations*. Similar findings were obtained for a variety of glass-formers [20,33,34,37,48].

It was shown that it is possible to take account of the excess contributions in the minimum region by adding further constant-loss or power-law terms to equation (9) [33,34,59]. However, the development of a theoretical base for these contributions [102] is in its beginning stages only.

In the frustration-limited domain (FLD) model by Kivelson, Tarjus, and coworkers [23] a 'narrowly avoided critical point' at a temperature T* above the melting point is postulated. The theory is based on the assumption that there is a locally preferred structure (LPS) which, however, is not able to tile space periodically. Without this geometrical constraint the system would condense into the LPS at T*. In real systems somewhat below T*, frustration-limited domains with the LPS are formed. Such a scenario is intuitive for the simple system of spherical molecules. Here the LPS is an icosahedral short-range order but one cannot tile space with this structure. In the FLD model [23] the $\alpha$-relaxation is identified with the restructuring of the FLDs and occurs on a length scale given by their characteristic size. Within the FLD framework there is a second length scale, the correlation length $\xi$ of the locally preferred structure. It was argued [23] that the experimentally observed fast $\beta$-processes may be ascribed to fast relaxations taking place on this smaller length scale of the FLD model. However, up to now a theoretical elaboration of the fast processes within FLD theory is missing.

**Figure 10. Dielectric loss of glycerol (*a*) and PC (*b*) in the minimum and boson peak region. The solid lines are fits with the MCT prediction, equations (10), with a= 0.325, b= 0.63 for glycerol and a= 0.29, b= 0.5 for PC. For the lowest temperatures, the increase towards the boson peak approaches power laws $\varepsilon'' \sim \nu^3$ for glycerol and $\varepsilon'' \sim \nu$ for PC as indicated by the dashed lines. Note that, in contrast to PC, the boson peak seems to be superimposed to the shallow minimum in glycerol. The dotted line in (b) is drawn to guide the eyes. The insets demonstrate for two temperatures each, that the simple superposition ansatz, equation (9), is not sufficient to explain the shallow minimum.**

Another model predicting fast processes is the CM of Ngai and coworkers [22]. Within this framework, the molecular units are predicted to exhibit a transition from an exponential fast relaxation to a slower KWW relaxation due to the onset of cooperative motion at a crossover time $t_c$. Continuity of the relaxing function (e.g. the polarization) at $t_c$ implies a correlation of the relaxation times of both processes and the relaxation time of the fast process can be calculated from the KWW parameters of the $\alpha$-process. For glycerol and PC [37], the fast process inherent in the CM is located at much lower frequencies than the $\varepsilon''(\nu)$-minimum and therefore cannot be invoked for the explanation of the excess intensity in this region.

Recently, a model was proposed considering a low-frequency relaxation-like part of the vibration susceptibility function, assumed to be responsible for the boson peak [103]. This relaxation-like response was shown to arise from anharmonicity of vibrations and invoked to explain the quasielastic line seen in light and neutron scattering. This quasielastic contribution corresponds to the fast $\beta$-relaxation region seen in the susceptibility spectra. Within this framework, the fast process should show up as peak with $\varepsilon'' \sim \nu^{\alpha}$ and $\varepsilon'' \sim \nu^{-1}$ at its low and high frequency side, respectively. For the absolute value of the exponent $\alpha$, reasonable values ranging between 0.375 and 1 were given in [103], depending on the system. No peak is seen between $\alpha$- and boson peak in the spectra of glycerol and PC (figure 10), but the $\nu^{-1}$-wing of the fast $\beta$-process may be obscured by the dominating boson peak at higher frequencies. Indeed, the spectra in glycerol give the impression of a boson peak with a steep ($\sim \nu^3$) low-frequency wing, superimposed to a shallow minimum (see section 6.3). In contrast, in PC a smooth transition of $\varepsilon''(\nu)$ from the minimum to the boson peak with only one power law ($\sim \nu^n$, $n \leqslant 1$) is observed, which seems unlikely to result from the superposition of the $\nu^a$-wing of the fast $\beta$-process and the low frequency wing of the boson peak (steeper than $\nu^1$, see above).

Very recently, by extending the Weiss mean-field theory to finite systems (clusters) and combining it with a model for the size dependence of the relaxation rate [24], it was possible to explain a considerable part of the present spectra of glycerol, including the $\varepsilon''(\nu)$-minimum [25,104]. Within this framework it is assumed that the basic thermodynamic units, the so-called aggregates, are subdivided into strongly interacting clusters which are statistically indistinguishable. From the distribution of the aggregate sizes and the size dependence of the relaxation rate of particles in an aggregate, a non-Debye $\alpha$-peak and an excess wing are predicted. In addition, peaks or shoulders can arise at high frequencies due to the fact that only integer values of m, the number of molecules per cluster, are possible. That is, these high-frequency features reflect the dynamic response of dimers, trimers, quadrimers, etc. [104].

The prediction of non-trivial additional contributions in the region of the $\varepsilon''(\nu)$-minimum is one of the main outcomes of the MCT. Within idealized MCT, for T above but near $T_c$, the minimum region can be approximated by the sum of two power laws [18]:

$$\varepsilon'' = \frac{\varepsilon_{\min}}{a+b}\left[a\left(\frac{\nu}{\nu_{\min}}\right)^{-b} + b\left(\frac{\nu}{\nu_{\min}}\right)^{a}\right] \qquad (10)$$

$\nu_{\min}$ and $\varepsilon_{\min}$ denote position and amplitude of the minimum, respectively. The power law $\nu^{-b}$ is often referred to as the von-Schweidler law, the power law $\nu^a$ as the critical law. Within MCT, the temperature independent exponents a and b are both related to each other by the exponent parameter $\lambda$ [18] and the exponent a is restricted to values below 0.4. Thus a significantly sublinear increase of $\varepsilon''(\nu)$ at frequencies above the minimum is predicted. Within MCT, the minimum region is denoted as the $\beta$-relaxation window. This is somewhat confusing as conventional relaxation contributions lead to peaks in $\varepsilon''(\nu)$. In addition, some confusion may arise with the (*slow*) Johari-Goldstein $\beta$-relaxations (section 2.2) and therefore often the term *fast* $\beta$-relaxation is used for the MCT process.

For PC, a consistent description of the $\varepsilon''(\nu)$-minima at $T \geqslant 193$ K is possible with $\lambda = 0.78$ ($a = 0.29$, $b = 0.5$) [34,37] (solid lines in figure 10b). The obtained $\lambda$ agrees reasonably with the results from other measurement techniques [78,105,106] and a very recent analysis of the present results in PC using a schematic two-correlator model within the framework of extended MCT [107]. The fits in figure 10b provide a good description of the data from 1–2 decades below $\nu_{\min}$ up to the boson peak frequency. The critical law clearly shows up between $\nu_{\min}$ and the boson peak frequency. In contrast, the von-Schweidler law is less well developed. The deviations of data and fits, seen at low frequencies in figure 10b, can be ascribed to the growing importance of the $\alpha$-relaxation. The simple interpolation formula, equation (10), is only valid in vicinity of the minimum. In contrast to PC, in glycerol (solid lines in figure 10a) the critical law is not well developed. Instead the MCT fits [33,34] are limited at high frequencies by the additional steeper increase towards the boson peak, not taken into account by the MCT expression (10). In PC this contribution seems to be of lower importance (see section 6.3). However, from figure 10a it seems reasonable that in glycerol position and height of the minimum determined from the fits is only weakly influenced by these contributions. Also the von-Schweidler law seems to extend nearly down to the $\alpha$-peak frequency. For glycerol an evaluation of the light and neutron scattering results with idealized MCT is hampered by the much stronger boson peak contribution (see section 6.2). However, in [65] light scattering results [73] were analysed using

a more sophisticated MCT approach including the boson peak. The value $\lambda = 0.73$ (a = 0.314, b = 0.591) obtained from this analysis is of similar magnitude as $\lambda = 0.705$ (a = 0.325, b = 0.63) deduced from the present dielectric results. The critical temperature $T_c$ should manifest itself in the temperature dependence of the $\varepsilon''(\nu)$-minimum. For $T > T_c$, the idealized MCT predicts the following relations:

$$\nu_{\min} \sim (T - T_c)^{1/(2a)} \tag{11}$$

$$\varepsilon_{\min} \sim (T - T_c)^{1/2} \tag{12}$$

But also the $\alpha$-relaxation timescale should exhibit critical behaviour:

$$\nu_\tau \sim (T - T_c)^{\gamma} \text{ with } \gamma = \frac{1}{2a} + \frac{1}{2b}. \tag{13}$$

In figure 11, the temperature dependencies of $\varepsilon_{\min}$, $\nu_{\min}$ and $\nu_\tau$ (same data as in figures 7 and 8) are shown. Here representations have been chosen that, according to equations (11), (12) and (13), should lead to straight lines extrapolating to $T_c$. Indeed, for both materials all three data sets can be described consistently with a $T_c \approx 187$ K for PC [34,37] and $T_c \approx 262$ K for glycerol [33,34] as indicated by the solid lines. But clearly, only the plots $\varepsilon_{\min}{}^2(T)$ for glycerol and $\nu_\tau{}^{1/\gamma}(T)$ for PC are really convincing. For PC, $T_c$ lies within the range of $T_c$ = 176–200 K, determined from various other techniques [78,89,106,108]. Also the recent, more sophisticated analysis of the present results in PC revealed a $T_c$ of 179 K [107]. For glycerol, from an analysis of light scattering results [73], in [65] a $T_c$ lying between 223 and 233 K was stated, clearly lower than the present value. For temperatures near $T_c$, especially for glycerol the data partly deviate from the predicted behaviour (figure 11). Within MCT this can be ascribed to a smearing out of the critical behaviour due to hopping processes which are considered in extended versions of MCT [17,18]. While somewhat above $T_c$ the relations (11), (12) and (13) should hold, critical laws are well known to fail too far above $T_c$. Therefore the proper choice of the temperature range to be used for the determination of $T_c$ is difficult which may lead to some uncertainties concerning the value of $T_c$.

Finally, it should be mentioned that idealized MCT predicts a significant change in the behaviour of $\varepsilon''(\nu)$ at $T_c$. For $T < T_c$, $\varepsilon''(\nu)$ should exhibit a so-called 'knee' at a frequency $\nu_k$ [18]. This knee should show up as a change of power law from $\varepsilon'' \sim \nu^a$ at $\nu > \nu_k$ to $\varepsilon'' \sim \nu$ at $\nu < \nu_k$. The quantities $\nu_k$ and the amplitude at the knee, $\varepsilon_k''$, should also exhibit critical behaviour. Using neutron and light scattering, various glass-formers were inspected for the presence of this unusual feature and there was considerable controversy in literature concerning its presence or absence [30,109,110]. In the present results for glycerol no indication of a knee is observed. The slight curvature seen, e.g. in the 183 K curve of PC near $10^{11}$ Hz (figure 10b) is not of sufficient significance to give evidence of a knee in this material. In [110] the absence of the knee was ascribed to hopping processes which are not included in idealized MCT.

### 6.2. *Comparison with other methods*

There is a variety of experimental investigations of the high-frequency response (in the GHz–THz region) of glass-forming materials using neutron and light scattering techniques [see e.g. 19–21,60,73,78]. The fluctuation-dissipation theorem [61] relates the measured intensity spectra to the imaginary part of a corresponding susceptibility, $\chi''$. The present high-frequency dielectric results for the first time allowed for a comparison of the dielectric susceptibility with that determined from the scattering experiments [32,33,36,37,47,111].

In figure 12 the dielectric loss spectra of glycerol and PC are compared with the imaginary part of the susceptibility, determined from neutron and light scattering data [73,78,112]. With the succession of $\alpha$-peak, minimum and boson peak the dielectric and light scattering results are qualitatively similar. The frequency range of the neutron scattering results is somewhat restricted but the minimum is seen nicely. As the scattering results give no information on the absolute magnitudes of $\chi''$, the data sets have been

**Figure 11. Temperature dependence of the amplitude $\varepsilon_{\min}$ (*a*, *d*) and position $\nu_{\min}$ (*b*, *e*) of the $\varepsilon''(\nu)$-minimum and of the $\alpha$-relaxation rate $\nu_\tau$ (*c*, *f*) of glycerol and PC. $\varepsilon_{\min}$ and $\nu_{\min}$ have been taken from the fits with equation (10), shown in figure 10. Representations have been chosen that should result in straight lines according to the predictions of the MCT, equations (11), (12) and (13). The solid lines demonstrate a consistent extrapolation for all three quantities to a $T_c$ of 262 K for glycerol and 187 K for PC.**

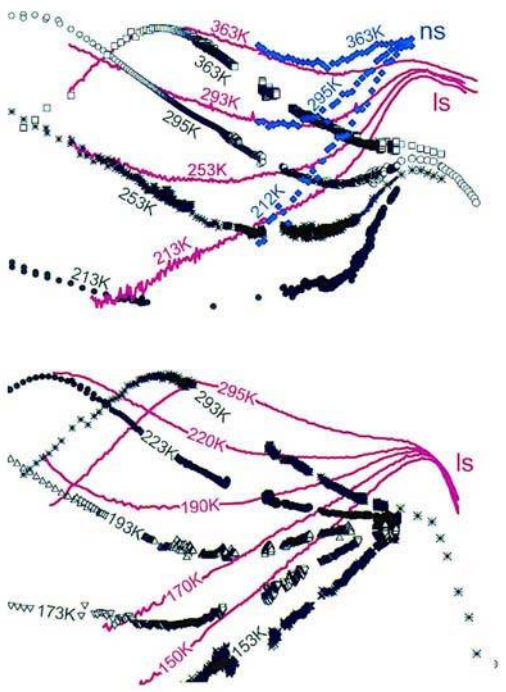


**Figure 12. Frequency dependence of the the imaginary part of the susceptibility, determined from dielectric (black symbols, present work, identical with $\varepsilon''$), light scattering (red lines, from [73,112] for glycerol, from [78] for PC) and neutron scattering measurements (blue diamonds, from [73,112] for glycerol only). The light and neutron scattering data sets have been vertically shifted to give a comparable intensity of the $\alpha$-peak. Note the different ratios of $\alpha$-peak and boson peak intensity and the different minimum positions.**

approximately scaled to yield a comparable height of the $\alpha$-peak. It should be mentioned that there is no rationale for this and a scaling, aiming at an equal height of the THz peak may be justified as well.

In figure 12a the $\alpha$-peak from light scattering and dielectric spectroscopy can be compared directly for glycerol at 363 K. It is located at the same frequency for both methods. In contrast, for PC it becomes obvious from figure 12b that the $\alpha$-peaks from dielectric spectroscopy are located at a significantly lower frequency. For both materials the $\alpha$-peak determined from light scattering is broader and exhibits a larger asymmetry. For glycerol it is well established that different methods as dielectric spectroscopy, specific heat spectroscopy, ultrasonics, and light scattering lead to very similar $\alpha$-relaxation times [83,113]. This may be rationalized by considering the presence of hydrogen bonds between neighbouring molecules in this material which should lead to a strong coupling of reorientational and translational motions of the molecules. In contrast, in the van-der-Waals bonded glass-former PC there is a difference in the absolute values of the $\alpha$-relaxation times determined from different experimental methods [78] indicating a decoupling of reorientational and translational degrees of freedom. However, the different relaxation times exhibit a common temperature behaviour, i.e. can be transferred into each other by a temperature independent factor [78]. This finding is in agreement with the prediction of MCT that in equation (13) only the prefactor should depend on the experimental probe.

For both materials, the increase towards the boson peak and its frequency position is almost identical for all experimental methods (figure 12). However, the ratio of the amplitudes of $\alpha$- and boson peak is much higher for the dielectric results. A similar behaviour was also found in our experiments on Salol [47] and in numerical molecular-dynamics simulations of various glass-forming systems [114–116]. Also the results from a very recent neutron scattering study of PC [106] indicate a much smaller ratio of $\alpha$- and boson peak amplitude than found in dielectric spectra. In addition, the position of the minimum differs between the different methods, also in accordance with results from molecular dynamics simulations [115,116]. An explanation for the differences between the dielectric and the light scattering susceptibilities was given by considering the different tensorial properties of the experimental probes [116].

It is one of the main predictions of MCT [18] that the same parameters $T_c$ and $\lambda$ should arise from all observables coupling to the density fluctuations. This is indeed the case for PC and may be also fulfilled for glycerol (see section 6.1). In addition, in contrast to the findings of figure 12, the position of the $\varepsilon''$- and $\chi''(\nu)$-minima should be the same, independent of the experimental method. MCT in its original form does not take account of non-spherical molecules and orientational degrees of freedom (ODF). However, dielectric spectroscopy and also light scattering experiments [117] primarily probe the orientational dynamics of the molecules and it may be suspected that ODFs play a role in the observed differences of the spectra from different methods. In this context it is of interest that for the ion-conducting glass-former $[Ca(NO_3)_2]_{0.4}[KNO_3]_{0.6}$ a rather good agreement of the minimum position from different experimental methods was found [111]. Here ODFs are not important and all experimental methods can be assumed to couple to translational modes. Recently some generalizations of MCT incorporating ODFs were proposed [118,119]. Indeed the larger ratio of $\alpha$- and microscopic-peak amplitude for $\varepsilon''$ in comparison to $\chi''$ from scattering experiments (figure 12) can be explained in this way [119]. However, this is not the case for the different positions of the minimum. But very recently an analysis of the present results and those from light and neutron

scattering, using a schematic two-correlator model within the framework of extended MCT, revealed that the hopping processes considered in extended MCT can lead to different minimum positions [107].

### 6.3. *Boson peak*

A variety of explanations of the boson peak has been proposed, e.g. in terms of the soft potential model [62], phonon localization models [63], or a model of coupled harmonic oscillators with a distribution of force constants [64]. Also MCT includes contributions leading to a peak at THz as was shown using a schematic two-correlator model [65]. While it seems likely that vibrational excitations are responsible for the boson peak, until now no consensus on a detailed microscopic explanation of this feature has been achieved. In the light of the restricted database in the THz frequency region it cannot be within the scope of the present work to compare the experimental results with the various model predictions. However, some interesting experimental facts shall be emphasized. As mentioned in sections 3 and 6.1, there is a significant difference of the spectra of glycerol and PC in the region between the minimum and the boson peak (figures 5 and 12): Here for PC only one power law, $\varepsilon'' \sim \nu^{a}$, is seen forming simultaneously the high frequency wing of the minimum and the low frequency wing of the boson peak. For $T \to T_g$, a linear behaviour is approached as indicated by the dashed line in figure 10b. In marked contrast, for glycerol two regimes can be distinguished: Just above $\nu_{min}$, there is a rather shallow increase of $\varepsilon''(\nu)$ which at high temperatures can be described by the critical law of MCT (figure 10a). But at higher frequencies a very steep increase appears, approaching $\varepsilon'' \sim \nu^{3}$ for $T \to T_g$ (dashed line in figure 10a). A similar characteristic is also seen in the light-scattering susceptibilities of both materials (figure 12). It seems that in glycerol the shallow minimum in $\varepsilon''(\nu)$ is obscured at high frequencies by a strong boson peak contribution and this is not the case for PC. This reasoning seems to be in accord with the empirical finding by Sokolov *et al.* [120] of a higher amplitude-ratio of boson peak and fast process for stronger glass formers (section 4.1). However, it has to be noted that in the present results, at least near $T_g$, this ratio, e.g. measured by comparing boson peak and minimum amplitude, is quite similar for both materials.

As mentioned in section 6.1, for glycerol, the presence of two distinct regions below the boson peak might be in accord with a model by Novikov [103], ascribing them to the relaxation-like and the main part of the vibrational excitations. Different relative boson peak strengths also explain the good fits with MCT up to the boson peak frequency in PC and the restricted validity of these fits at high frequencies in glycerol (figure 10). Interestingly, the light scattering results in glycerol, showing quite similar characteristics as the dielectric data (figure 12), were successfully described using a schematic two-correlator MCT model [65]. Further theoretical work is necessary to show if MCT is able to provide an explanation for all differences of the glycerol and PC dielectric spectra.

## 7. Summary and conclusions

The combination of a large variety of dielectric and optic techniques allows us to obtain spectra of the dielectric permittivity of glass-forming materials covering more than 18 decades of frequency. In the presented dielectric-loss spectra of two prototypical molecular glass formers, four different contributions can be clearly distinguished: the $\alpha$-peak, the excess wing, the minimum, and the boson peak. Only by dielectric spectroscopy is it possible to follow the development of all these features, starting from the glass region, near $T_g$, well up to temperatures deep in the liquid state.

It is an astonishing property of glass-forming materials that a dynamic process (the $\alpha$-relaxation) changes its time scale continuously over many decades with temperature (more than 15 decades in the present materials). Consequently, most theoretical approaches of the glass transition have concentrated on the description of the $\alpha$-relaxation time. Indeed the present results can be well described by various, partly very different, phenomenological and theoretical models [37]. The extension of the spectra to exceptionally high frequencies allows for a reliable determination of the high-temperature development of the $\alpha$-peak width parameter, which is a measure for the microscopic heterogeneity of the considered glass former [42–44]. For both glass formers investigated, it has a tendency to saturate at a finite non-Debye value at high temperatures. This result is of relevance concerning theoretical predictions of the MCT [18] and may help to resolve the apparent discrepancy of the results from dielectric and other measurements. However, overall it has to be concluded that it is difficult to arrive at a final decision in favour of or against a specific model on the dynamics of glass-forming materials from an evaluation of the $\alpha$-relaxation alone.

The excess wing, well developed in glycerol and PC, follows the scaling, demonstrated by Nagel and coworkers [52] to collapse dielectric spectra of various glass formers, collected at different temperatures, onto one master curve. At the highest frequencies some small deviations from a single master curve may be suspected, a finding which deserves further investigation. If a general failure of the Nagel-scaling should show up, the excess wing may be not so intimately related to the $\alpha$-relaxation as thought up to now and the view of the excess wing as independent process, e.g. a $\beta$-relaxation, may be corroborated. In addition, the data were checked for a possible crossover

to a constant loss at low temperatures which could imply a divergence of the static susceptibility, proposed recently [53]. Indeed, the experimental data, especially the wing exponent b(T) seem to be consistent with this assumption. However, in our opinion the present dielectric data and those reported in literature are far from providing a convincing proof for a divergent susceptibility at low temperatures.

Possibly the most important outcome of these broad-band dielectric experiments is the presence of additional intensity in the region of the $\varepsilon''(\nu)$-minimum, in the GHz–THz frequency range. Clearly, fast processes have to be invoked to explain its spectral form. The minimum can well be described by the sum of power laws and a constant loss [59], but possible theoretical explanations for these contributions are still in their beginning stages. The model by Novikov [103], considering the fast $\beta$-processes as relaxation-like part of vibrational excitations, seems to be in qualitative accord with the results in glycerol but in disagreement with the spectra of PC. The MCT provides a microscopic explanation for the fast $\beta$-processes in both materials. A quantitative agreement of the model predictions of idealized MCT and the spectra in the minimum region is found for high temperatures, however, restricted in glycerol to frequencies below the additional steep boson peak contribution. For low temperatures, towards $T_g$, at least a qualitative agreement with MCT predictions can be stated, but more work is needed for a quantitative comparison. Indeed, very recently a great step forward was made in the quantitative theoretical explanation of the complete spectra in PC within the framework of MCT [107].

In contrast to PC, in glycerol the shallow minimum seems to be superimposed by a very steep boson peak, which may be correlated with the smaller 'fragility' [82] (see section 4.1) of this glass former [120]. It can be speculated that the 'boson peak' seen in PC may be of different origin than the boson peak in glycerol. Interestingly, in some materials there are indications for *two* superimposed peaks in the THz region [e.g. 20,60].

In summary, in the present dielectric results many of the characteristic, so far unexplained, properties of glass-forming materials show up: the non-Arrhenius $\alpha$-relaxation time, the excess wing with its intriguing scaling property, the additional intensity in the minimum region, and the boson peak. None of the presented theories is able to take account of all of those experimental observations. However, in our judgement MCT provides the most consistent picture providing explanations for the largest variety of experimental facts, including the high-frequency processes. Admittedly, alternative explanations may be possible. Also many questions need to be addressed in more detail, e.g. the behaviour below $T_c$, the differences of dielectric and scattering results and the qualitatively different behaviour of PC and glycerol in the boson peak region. But also more experimental work is needed, e.g. concerning the boson peak region and the filling of the 'gaps' in the GHz region at low temperatures. Nevertheless, the recent tremendous theoretical and experimental progress in the field of glass physics let us hope that these and other open questions will be solved in due course, finally arriving at a consistent picture of the glass transition and dynamics in the near future.

**Acknowledgements**

We gratefully acknowledge stimulating discussions with C. A. Angell, R. Böhmer, R. V. Chamberlin, H. Z. Cummins, M. Fuchs, W. Götze, K. L. Ngai, W. Petry, R. Schilling, W. Schirmacher, L. Sjögren, A. P. Sokolov, Th. Voigtmann, and J. Wuttke. We thank M. Ohl and J. Wuttke for information on the results of the neutron scattering experiments of ref. [106] and W. Götze and Th. Voigtmann for information on their MCT analysis of the PC spectra prior to publication. We are indebted to H. Z. Cummins and J. Wuttke for providing the published light and neutron scattering results shown in figure 12. We thank M. Dressel, Yu. G. Goncharov, B. Gorshunov, A. Pimenov, and B. Schiener for help in the dielectric measurements and are obliged to Th. Wiedenmann for technical support. This work was supported by the Deutsche Forschungsgemeinschaft, Grant-No. LO264/8-1 and partly by the BMBF, contract-No. 13N6917.

**References**

[1] Zarzycki, J., 1991, *Glasses and the vitreous state* (Cambridge: Cambridge University Press).

[2] Cable, M., 1991, in *Materials Science and Technology , Vol. 9, Glasses and Amorphous Materials*, edited by J. Zarzycki (Weinheim: VCH), pp. 1–89.

[3] Storey, K. B., and Store, J. M., 1990, *Scientific American*, December, 62–67.

[4] Anderson, P. W., 1995, *Science*, **267,** 1615–1616.

[5] Ediger, M. D., Angell, C. A., and Nagel, S. R., 1996, *J. Phys. Chem.*, **100,** 13200–13212.

[6] Arguments against the common belief that medieval glass has changed its shape over the centuries are advanced by: Zanotto, E. D., 1998, *Am. J. Phys.*, **66,** 392–395; Zanotto, E. D., and Gupta, P. K., 1999, *Am. J. Phys.*, **67,** 260–262.

[7] Bible, Book of Judges, Ch. 5, Verse 5 (the translation of the Hebrew text is somewhat equivocal here: the English translation reads 'the mountains melted' while the Latin translation reads 'montes fluxerunt').

[8] Vogel, H., 1921, *Phys. Z.*, **22,** 645–646; Fulcher, G. S., 1925, *J. Am. Ceram. Soc.*, **8,** 339–355; Tammann, G., and Hesse, W., 1926, *Z. Anorg. Allg. Chem.*, **156,** 245–257.

[9] Leheny, R. L., and Nagel, S. R., 1998, *Phys. Rev.* B, **57,** 5154–5162.

[10] Kauzmann, W., 1942, *Rev. Mod. Phys.*, **14,** 12–44.

[11] Zallen, R., 1983, *The Physics of Amorphous Solids*, (New York: John Wiley & Sons); Elliott, S. R., 1990, *Physics of Amorphous Materials* (London: Longman Scientific & Technical).

[12] Adam, G., and Gibbs, J. H., 1965, *J. Chem. Phys.*, **43,** 139 – 146.
[13] For a review of various theories of the glass transition, see: Jäckle, J., 1986, *Rep. Prog. Phys.*, **49,** 171 – 231.
[14] Cohen, M. H., and Turnbull, D., 1959, *J. Chem. Phys.*, **31,** 1164 – 1169.
[15] Cohen, M. H., and Grest, G. S., 1979, *Phys. Rev. B*, **20,** 1077 – 1098; Grest, G. S., and Cohen, M. H., 1981, *Adv. Chem. Phys.*, **48,** 455 – 525.
[16] Bengtzelius, U., Götze, W., and Sjölander, A., 1984, *J. Phys. C*, **17,** 5915 – 5934; Leutheuser, E., 1984, *Phys. Rev. A*, **29,** 2765 – 2773; Götze, W., 1985, *Z. Phys. B*, **60,** 195 – 203.
[17] Götze, W., and Sjögren, L., 1987, *Z. Phys. B*, **65,** 415 – 427.
[18] For reviews of MCT, see: Götze, W., and Sjögren, L., 1992, *Rep. Progr. Phys.*, **55,** 241 – 376; Schilling, E., 1994, in: *Disorder Effecs on Relaxational Properties*, edited by R. Richert and A. Blumen (Berlin: Springer), pp. 193 – 231; Cummins, H.Z., 1999, *J. Phys.: Cond. Matter*, **11,** A95 – A117.
[19] For a review of neutron scattering results, see: Petry, W., and Wuttke, J., 1995, *Transp. Theory Statist. Phys.*, **24,** 1075 – 1095.
[20] A critical comparison of various recent experimental results on glass formers with a variety of theoretical predictions is given in: Cummins, H. Z., Li, G., Hwang, Y. H., Shen, G. Q., Du, W. M., Hernandez, J., and Tao, N. J., 1997, *Z. Phys. B*, **103,** 501 – 519.
[21] For a review of experimental tests of MCT, see: Götze, W., 1999, *J. Phys.: Cond. Matter*, **10A,** 1 – 45.
[22] Ngai, K. L., 1979, *Comments Solid State Phys.*, **9,** 127 – 140; Ngai, K. L., 1994, in: *Disorder Effects on Relaxational Properties*, edited by R. Richert and A. Blumen (Berlin: Springer), p. 89 – 150; Ngai, K. L., and Rendell, R. W., 1997, in *Supercooled Liquids, Advances and Novel Applications*, edited by J. T. Fourkas, D. Kivelson, U. Mohanty, and K. A. Nelson, *ACS Symposium Series Vol. 676* (Washington, DC, American Chemical Society), pp. 45 – 66.
[23] Kivelson, D., Kivelson, S. A., Zhao, X-L., Nussinov, Z., and Tarjus, G., 1995, *Physica A*, **219,** 27 – 38; Tarjus, G., Kivelson, D., and Kivelson, S., 1997 in *Supercooled Liquids, Advances and Novel Applications*, edited by J. T. Fourkas, D. Kivelson, U. Mohanty, and K. A. Nelson, *ACS Symposium Series Vol. 676* (Washington, DC, American Chemical Society), pp. 67 – 81.
[24] Chamberlin, R. V., 1993, *Phys. Rev. B*, **48,** 15638 – 15645.
[25] Chamberlin, R. V., 1999, *Phys. Rev. Lett.* **82,** 2520 – 2523.
[26] Johari, G. P., and Goldstein, M., 1970, *J. Chem. Phys.*, **53,** 2372 – 2388.
[27] Johari, G. P., 1976, in *The Glass Transition and the Nature of the Glassy State*, edited by M. Goldstein and R. Simha [*Ann. New York Acad. Sci.*, **279,** 117 – 140].
[28] Ngai, K.L., Cramer, C., Saatkamp, T., and Funke, K., 1996, in *Proceedings of the Workshop on Non-Equilibrium Phenomena in Supercooled Fluids, Glasses, and Amorphous Materials, Pisa, Italy, 1995*, edited by M. Giordano *et al.* (Singapore: World Scientific), pp. 3 – 21.
[29] Schönhals, A., Kremer, F., Hofmann, A., Fischer, E. W., and Schlosser, E., 1993, *Phys. Rev. Lett.*, **70,** 3459 – 3462.
[30] Dixon, P. K., Menon, N., and Nagel, S. R., 1994, *Phys. Rev E*, **50,** 1717 – 1719.
[31] Hofmann, A., Kremer, F., Fischer, E. W., and Schönhals, A., 1994, in *Disorder Effects on Relaxational Processes*, edited by R. Richert and A. Blumen (Berlin: Springer), pp. 309 – 331.
[32] Pimenov, A., Lunkenheimer, P., Rall, H., Kohlhaas, R., Loidl, A., and Böhmer, R., 1996, *Phys. Rev. E*, **54,** 676 – 684.
[33] Lunkenheimer, P., Pimenov, A., Dressel, M., Goncharov, Yu. G., Böhmer, R., and Loidl, A., 1996, *Phys. Rev. Lett.*, **77,** 318 – 321.
[34] Lunkenheimer, P., Pimenov, A., Dressel, M., Gorshunov, B., Schneider, U., Schiener, B., and Loidl, A., 1997, in *Supercooled Liquids, Advances and Novel Applications*, edited by J. T. Fourkas, D. Kivelson, U. Mohanty, and K. A. Nelson, *ACS Symposium Series Vol. 676* (Washington, DC, American Chemical Society), pp. 168 – 180.
[35] Lunkenheimer, P., Pimenov, A., and Loidl, A., 1997, *Phys. Rev. Lett.*, **78,** 2995 – 2998.
[36] Schneider, U., Lunkenheimer, P., Brand, R., and Loidl, A., 1998, *J. Non-Cryst. Solids*, **235 – 237,** 173 – 179.
[37] Schneider, U., Lunkenheimer, P., Brand, R., and Loidl, A., 1999, *Phys. Rev. E*, **59,** 6924 – 6936.
[38] Böttcher, C. J. F., and Bordewijk, P., 1978, *Theory of Electric Polarization, Vol. II* (Amsterdam: Elsevier).
[39] Debye, P., 1912, *Phys. Z.*, **3,** 97 – 100; Debije, P., 1913, *Ber. D. Phys. Ges.*, **16,** 777 – 789.
[40] Davidson, D. W., and Cole, R. H., 1950, *J. Chem. Phys.*, **18,** 1417; Davidson, D. W., and Cole, R. H., 1951, *J. Chem. Phys.*, **19,** 1484 – 1490.
[41] For a review on heterogeneity in glass-forming liquids, see: Sillescu, H., 1999, *J. Non-Cryst. Solids*, **243,** 81 – 108.
[42] Schmidt-Rohr, K., and Spiess, H. W., 1991, *Phys. Rev. Lett.*, **66,** 3020 – 3023; Böhmer, R., Hinze, G., Diezemann, G., Geil, B., and Sillescu, H., 1996, *Europhys. Lett.*, **36,** 55 – 60.
[43] Schiener, B., Böhmer, R., Loidl, A., and Chamberlin, R. V., 1996, *Science* **274,** 752 – 754.
[44] Cicerone, M. T., and Ediger, M. D., 1995, *J. Chem. Phys.*, **103,** 5684 – 5692.
[45] Kohlrausch, R., 1854, *Ann. Phys.*, **167,** 56 – 82; ibid., 179 – 214.
[46] Williams, G., and Watts, D. C., 1970, *Trans. Faraday Soc.*, **66,** 80 – 85.
[47] Lunkenheimer, P., Pimenov, A., Dressel, M., Gorshunov, B., Schneider, U., Schiener, B., Böhmer, R., and Loidl, A., 1997, in *Structure and Dynamics of Glasses and Glass Formers*, edited by C. A. Angell, K. L. Ngai, J. Kieffer, T. Egami, and G. U. Nienhaus, *MRS Symposium Proceedings Vol. 455* (Pittsburgh: Material Research Society), pp. 47 – 57.
[48] Brand, R., Lunkenheimer, P., and Loidl, A., *Phys. Rev. B*, **56,** R5713 – 5716.
[49] Lunkenheimer, P., Pimenov, A., Schiener, B., Böhmer, R., and Loidl, A., 1996, *Europhys. Lett.*, **33,** 611 – 616.
[50] Leheny, R. L., and Nagel, S. R., 1997, *Europhys. Lett.*, **39,** 447 – 452.
[51] Kudlik, A., Benkhof, S., Blochowicz, T., Tschirwitz, C., and Rössler, E., 1999, *J. of Molecular Structure*, **479,** 201 – 218.
[52] Dixon, P. K., Wu, L., Nagel, S. R., Williams, B. D., and Carini, J. P., 1990, *Phys. Rev. Lett.*, **65,** 1108 – 1111.
[53] Menon, N., and Nagel, S. R., 1995, *Phys. Rev. Lett.*, **74,** 1230 – 1233.
[54] Ngai, K. L., 1998, *Phys. Rev. E*, **57,** 7346 – 7349; Ngai, K. L., 1998, *J. Chem. Phys.*, **109,** 6982 – 6994.
[55] León, C., and Ngai, K. L., 1999, *J. Phys. Chem.*, **103,** 4045 – 4051.
[56] Wagner, H., and Richert, R., 1999, *J. Chem. Phys.*, **110,** 11660 – 11663.
[57] Strom, U., Hendrickson, J. R., Wagner, R. J., and Taylor, P. C., 1974, *Solid State Commun.*, **15,** 1871 – 1875; Strom, U., and Taylor, P. C., 1977, *Phys. Rev. B*, **16,** 5512 – 5522.
[58] Wong, J., and Angell, C. A., *Glass: Structure by Spectroscopy* (New York: M. Dekker).
[59] Lunkenheimer, P., Schneider, U., Brand, R., and Loidl, A., 1999, in *Slow Dynamics in Complex Systems: Eighth Tohwa University International Symposium*, edited by M. Tokuyama and I. Oppenheim, *AIP Conf. Proc. No. 469* (New York, AIP), pp. 433 – 440.

[60] Rössler, E., Novikov, V. N., and Sokolov, A. P., 1997, *Phase Transitions*, **63,** 201 – 233.

[61] Lovesey, S. W., 1984, *Theory of Neutron Scattering from Condensed Matter, Volume 1* (Oxford: Clarendon Press), p. 301.

[62] Karpov, V. G., Klinger, M. I., and Ignatiev, F. N., 1983, *Sov. Phys. JETP*, **57,** 439 – 448; Buchenau, U., Galperin, Yu. M., Gurevich, V. L., Parshin, D. A., Ramos, M. A., and Schober, H. R., 1992, *Phys. Rev. B*, **46,** 2798 – 2808.

[63] Malinovsky, V. K., Novikov, V. N., and Sokolov, A. P., 1992, *J. Non-Cryst. Solids*, **90,** 485 – 488; Elliott, S. R., 1992, *Europhys. Lett.*, **19,** 201 – 206.

[64] Schirmacher, W., Diezemann, G., and Ganter, C., 1998, *Phys. Rev. Lett.*, **81,** 136 – 139.

[65] Franosch, T., Götze, W., Mayr, M. R., and Singh, A. P., 1997, *Phys. Rev. E*, **55,** 3183 – 3190.

[66] Böhmer, R., Schiener, B., Hemberger, J., and Chamberlin, R. V., 1995, *Z. Phys. B*, **99,** 91 – 99.

[67] Afsar, M. N., Birch, J. R., and Clarke, R. N., 1986, *Proc. IEEE*, **74,** 183 – 199; Wei, Y.-Z., and Sridhar, S., 1989, *Rec. Sci. Instrum.*, **60,** 3041 – 3046; Jenkins, S., Hodgetts, T. E., Clarke, R. N., and Preece, A. W., 1990, *Meas. Sci. Technol.*, **1,** 691 – 702; Moreau, J. M., and Aziz, R., 1993, *Meas. Sci. Technol.* **4,** 124 – 129; Ji, G. Q., Wong, W. H., Raskovich, E. Y., Clark, W. G., Hines, W. A., and Sanny, J., 1993, *Rev. Sci. Instrum.*, **64,** 1614 – 1621.

[68] Böhmer, R., Maglione, M., Lunkenheimer, P., and Loidl, A., 1989, *J. Appl. Phys.*, **65,** 901 – 904.

[69] Nicholson, A. M., and Ross, G. F., 1970, *IEEE Trans. Instrum. Meas.*, **IM-19**, 377 – 382.

[70] Volkov, A. A., Goncharov, Yu. G., Kozlov, G. V., Lebedev, S. P., and Prokhorov, A. M., 1985, *Infrared Phys.* **25,** 369 – 373; Volkov, A. A., Kozlov, G. V., Lebedev, S. P., and Prokhorov, A. M., 1989, *Infrared Phys.* **29,** 747 – 752.

[71] Born, M., and Wolf, E., 1980, *Principles of Optics* (Oxford: Pergamon Press).

[72] Wooten, F., 1972, *Optical Properties of Solids* (New York: Academic Press).

[73] Wuttke, J., Hernandez, J., Li, G., Coddens, G., Cummins, H. Z., Fujara, F., Petry, W., and Sillescu, H., 1994, *Phys. Rev. Lett.*, **72,** 3052 – 3055.

[74] Kudlik,A., 1997, PhD Thesis, Universität Bayreuth, Germany.

[75] Barthel, J., Bachhuber, K., Buchner, E., Gill, J. B., and Kleebauer, M., 1990, *Chem. Phys. Lett.*, **167,** 62 – 66.

[76] Huck, J. R., Noyel, G. A., Jorat, L. J., and Bondeau, A. M., 1982, *Journal of Electrostatics*, **12,** 221 – 228.

[77] Payne, R., and Theodorou, I. E., 1972, *J. Phys. Chem.*, **76,** 2892 – 2900.

[78] Du, W. M., Li, G., Cummins, H. Z., Fuchs, M., Toulouse, J., and Knauss, L. A., 1994, *Phys. Rev. E*, **49,** 2192 – 2205.

[79] Stickel, F., Fischer, E. W., and Richert, R., 1996, *J. Chem. Phys.*, **104,** 2043 – 2055.

[80] Angell, C. A., Boehm, L., Oguni, M., and Smith, D. L., 1993, *J. Molecular Liquids*, **56,** 275 – 286.

[81] Menon, N., O'Brian, K. P., Dixon, P. K., Wu, L., Nagel, S. R., Williams, B. D., and Carini, J. P., 1992, *J. Non-Cryst. Solids*, **141,** 61 – 65.

[82] Angell, C. A., 1985, in *Relaxations in Complex Systems*, edited by K. L Ngai, and G. B. Wright (Washington, DC: NRL), pp. 3 – 11; Böhmer, R., Ngai, K. L., Angell, C. A., and Plazek, D. J., 1993, *J. Chem. Phys.*, **99,** 4201 – 4209.

[83] Jeong, Y. H., Nagel, S. R., and Bhattacharya, S., 1986, *Phys. Rev. A*, **34,** 602 – 608.

[84] Dixon, P. K., 1990, *Phys. Rev. B*, **42,** 8179 – 8186; Cummins, H. Z., Li., G., Du, W. M., Hernandez, J., and Tao, N. Z., 1994, *J. Phys. Cond. Matter*, **6,** A51 – A62.

[85] Stickel, F., Fischer, E. W., and Richert, R., 1995, *J. Chem. Phys.*, **102,** 6251 – 6257.

[86] Stickel, F., Fischer, E. W., Schönhals, A., and Kremer, F., 1994, *Phys. Rev. Lett.*, **73,** 2936.

[87] Kivelson, D., Tarjus, G., Zhao, X., and Kivelson, S.A., 1996, *Phys. Rev. E*, **53,** 751 – 758.

[88] Li, G., Du, W. M., Sakai, A., and Cummins, H. Z., 1992, *Phys. Rev. A*, **46,** 3343 – 3356.

[89] Börjesson, L., Elmroth, M., and Torell, L. M., 1990, *Chem. Phys.*, **149,** 209 – 220.

[90] Rössler, E., Sokolov, A. P., Kisliuk, A., and Quitmann, D., 1994, *Phys. Rev. B*, **49,** 14967 – 14978.

[91] Yang, Y., and Nelson, K. A., 1996, *J. Chem. Phys.*, **104,** 5429 – 5435.

[92] Cheng, L.-T., Yan, Y.-X., and Nelson, K. A., 1989, *J. Chem. Phys.*, **91,** 6052 – 6061; Sidebottom, D. L., and Sorensen, C. M., 1989, *J. Chem. Phys.*, **91,** 7153 – 7158; Steffen, W., Patkowski, A., Gläser, H., Meier, G., and Fischer, E. W., 1994, *Phys. Rev. E*, **49,** 2992 – 3002.

[93] Stickel, F., 1995, PhD Thesis, Johannes Gutenberg-Universität Mainz (Germany).

[94] Lunkenheimer, P., 1999, unpublished.

[95] Menon N., and Nagel, S. R., 1993, *Phys. Rev. Lett.*, **71,** 4095; Schönhals, A., Kremer, F., and Stickel, F., 1993, *Phys. Rev. Lett.*, **71,** 4096; Leheny, R. L., Menon, N., and Nagel, S. R., 1996, *Europhys. Lett.*, **36,** 473 – 474; Kudlik, A., Blochowicz, T., Benkhof, S., and Rössler, E., 1996, *Europhys. Lett.*, **36,** 475 – 476.

[96] Schönhals, A., Kremer, F., and Schlosser, E., 1991, *Phys. Rev. Lett.*, **67,** 999 – 1002.

[97] Kudlik, A., Benkhof, S., Lenk, R., and Rössler, E., 1995, *Europhys. Lett.*, **32,** 511 – 516.

[98] Dendzik, Z., Paluch, M., Gburski, Z., and Zioto, J., 1997, *J. Phys.: Condens. Matter*, **9,** L339 – L346; Paluch, M., Dendzik, Z., and Gburski, Z., 1998, *J. Non-Cryst. Solids*, **232 – 234,** 390 – 395.

[99] Leslie-Pelecky, D. L., and Birge, N. O., 1994, *Phys. Rev. Lett.*, **72,** 1232 – 1235.

[100] Brand, R., Lunkenheimer, P., Schneider, U., and Loidl, A., 1999, *Phys. Rev. Lett.*, **82,** 1951 – 1954.

[101] Schneider, U., Brand, R., Lunkenheimer, P., and Loidl, A., 1999, submitted to Eur. Phys. J. B.

[102] Cole, R. H., and Tombari, E., 1991, *J. Non-Cryst. Solids*, **131 – 133**, 969 – 972; Ngai, K. L., Strom, U., and Kanert, O., 1992, *Phys. Chem. Glasses*, **33,** 109 – 115; Lim, B. S., Vaysleyb, A. V., and Nowick, A. S., 1993, *Appl. Phys. A*, **56,** 8 – 14; Elliott, S. R., 1994, *Solid State Ionics*, **70/71,** 27 – 40; Sidebottom, D. L., Green, P. F., and Brow, R. K., 1995, *J. Non-Cryst. Solids*, **203,** 300 – 305; Ngai, K. L., Jain, H., and Kanert, O., *J. Non-Cryst. Solids*, **222,** 383 – 390.

[103] Novikov, V. N., 1998, *Phys. Rev. B*, **58,** 8367 – 8378.

[104] Chamberlin, R. V., 1999, preprint; Chamberlin, R. V., private communication.

[105] Ma, J., Vanden Bout, D., and Berg, M., 1996, *Phys. Rev. E*, **54,** 2786 – 2797.

[106] Wuttke, J., Ohl, M., Goldammer, M., Roth, S., Schneider, U., Lunkenheimer, P., Kahn, R., Rufflé, B., Lechner, R., and Berg, M. A., 1999, submitted to *Phys. Rev. E*.

[107] Götze, W., Voigtmann, Th., private communication.

[108] Börjesson, L., and Howells, W. S., 1991, *J. Non-Cryst. Solids*, **131 – 132**, 53 – 57.

[109] Zeng, C. Z., Kivelson, D., and Tarjus, G., 1994, *Phys. Rev. E*, **50,** 1711 – 1716; Cummins, H.Z., and Li, G., 1994, *Phys. Rev. E*, **50,** 1720 – 1726; Gapinski, J, Steffen, W., Patkowski, A, Sokolov, A. P., Kisliuk, A., Buchenau, U., Russina, M., Mezei, F., and Schober, H., 1999, *J. Chem. Phys.*, **110,** 2312 – 2315.

[110] Barshilia, H. C., Li, G., Shen, G. Q., and Cummins, H.Z., *Phys. Rev. E*, **59,** 5625 – 5628.

[111] Lunkenheimer, P., Pimenov, A., Dressel, M., Schiener, B., Schneider, U., and Loidl, A., 1997, *Progr. Theor. Phys. Suppl.*, **126,** 123 – 131.
[112] Wuttke, J., private communication.
[113] Birge, N. O., 1986, *Phys. Rev. A*, **34,** 1631 – 1642; Ngai, K. L., and Rendell, R. W., 1990, *Phys. Rev. B*, **41,** 754 – 756; Wu, L., Dixon, P. K., Nagel, S. R., Williams, B. D., and Carini, J. P., 1991, *J. Non-Cryst. Solids*, **131 – 133,** 32 – 36.
[114] Wahnströhm, G., and Lewis, L. J., 1997, *Progr. Theor. Phys. Suppl.*, **126,** 261 – 266.
[115] Kämmerer, S., Kob, W., Schilling, R., 1998, *Phys. Rev. B*, **58,** 2141 – 2150.
[116] Lebon, M. J., Dreyfus, C., Guissani, Y., Pick, R. M., Cummins, H. Z., 1997, *Z. Phys. B*, **103,** 433 – 439.
[117] Cummins, H. Z., Li, G., and Du, W., 1996, *Phys. Rev. E*, **53,** 896 – 904.
[118] Franosch, T., Fuchs, M., Götze, W., Mayr, M. R., and Singh, A. P., 1997, *Phys. Rev. E*, **56,** 5659 – 5674.
[119] Schilling, R., and Scheidsteger, T., 1997, *Phys. Rev. E*, **56,** 2932 – 2949.
[120] Sokolov, A.P., Rössler, E., Kisliuk, A., and Quitmann, D., 1993, *Phys. Rev. Lett.*, **71,** 2062 – 2065.

*Peter Lunkenheimer* obtained his first degree in physics at the Johannes-Gutenberg Universität in Mainz (Germany) in the field of heavy fermion physics. His Ph.D. on the topic of the complex conductivity of high-$T_c$ superconductors was completed there 1992. During his stay at the Technische Hochschule Darmstadt (Germany) from 1992 – 1996 his main interest started to focus on glass physics. Since 1996 he is employed at the Universität Augsburg (Germany), where he is currently working at his Habilitation on the dynamic response of glass-forming liquids, investigated by broadband dielectric spectroscopy.

*Ulrich Schneider* completed his studies of physics with a diploma thesis on the ferroelectric Rochelle salt compounds at the Technische Hochschule Darmstadt in 1996. He is currently working on his Ph.D. in the Augsburg dielectric laboratory, concentrating on the high-frequency dynamics of molecular liquids.

*Robert Brand* obtained his diploma in physics at the Technische Hochschule Darmstadt in 1997. He is now working at the Universität Augsburg on his Ph.D. His main research interest are the plastic crystals as model systems for glass formers.

*Alois Loidl* graduated from the Technische Universität Wien (Austria) in 1971, with a diploma thesis on nuclear physics. He gained his Ph.D. at the Johann Wolfgang von Goethe Universität Frankfurt (Germany) 1976 and his Habilitation at the Johannes-Gutenberg Universtät Mainz in 1981. In Mainz he also had an assistance and associate professorship in solid state physics. From 1991 to 1996 he had a full professorship at the Technische Hochschule Darmstadt and since 1996 he holds a chair in experimental physics at the Universität Augsburg. His fields of interest are in the physics of disordered systems, in the broad field of electronically highly correlated systems, like heavy-fermion compounds, high-$T_c$ superconductors and in anomalous properties of transition metal oxides.